adjacent to clusters of the *CDKN2* and *IFNA* families, and is a well-known hotspot of genomic loss in several types of human cancers. We performed genome-wide scans of genetic lesions in 168 ATL samples and demonstrated that 21 ATL cases (12.5%) had genomic deletion of 9p21.3 containing the *hsa-miR-31* coding region (Figure 4A; Figure S3A). All of these cases also have genomic defect in *CDKN2A* region. A major proportion of ATL cases that are without genetic deletion and somatic mutation in the *hsa-miR-31* region showed remarkable loss of miR-31 expression (Figure 4B). Detailed expression profiling revealed drastic downregulation of *Pri-miR-31* transcription in the primary ATL cells (Figure 4C). There was a strong correlation between the levels of mature miR-31 and primary transcript ($r = 0.9414$, $p = 5.45 \times 10^{-8}$). *hsa-miR-31* is located in intronic region of *LOC554202* gene. However, *LOC554202* mRNA levels were very low in primary T cells and there was no significant difference between ATL and normal cells, strongly suggesting that loss of miR-31 expression is due to specific transcriptional suppression in ATL cells. Using computational analysis, we identified a putative TATA box and transcriptional start site (TSS) 2500 bp upstream of the miR-31 coding region (Figure 4D). Although no CpG islands were found in this region, we unexpectedly discovered an assembly of YY1-binding motifs upstream of the miR-31 region in human and mouse (Figure 4D; Figure S3C). YY1 is a pivotal transcription factor and a recruitor of the Polycomb repressive complex (PRC) (Simon and Kingston, 2009). Convergence of the YY1 binding sequence, especially the repressive motif (Figure S3D), seems to be evolutionarily conserved, suggesting that YY1 is important in the regulation of miR-31 transcription. We further performed chromatin immunoprecipitation (ChIP) to evaluate repressive histone hallmarks, including di- and trimethylated H3K9 (H3K9me2 and H3K9me3) and trimethylated H3K27 (H3K27me3). The results showed higher levels of methylation at H3K9 and H3K27 in a broad area containing the miR-31 coding region (Figure 4E). As shown in Figures S3E–S3G, there was an inverse correlation between the levels of miR-31 expression and repressive histone methylation. These data allowed us to hypothesize that histone methylation, especially that of Polycomb family-dependent H3K27me3, may contribute to miR-31 repression. To confirm our hypothesis, we performed a YY1 knockdown experiment using a specific shRNA (Figures 4F–4I). As expected, knockdown of YY1 led to an increase in the levels of *Pri-miR-31* and mature miR-31 (Figures 4F and 4G). Furthermore, ChIP assays showed that YY1 occupied the miR-31 region, especially in the upstream region of TSS, where there is an array of YY1 binding sites (Figures 4D and 4H). The results also demonstrated that decreased occupancy of YY1 and concomitant derecruitment of EZH2, a key component of PRC2, were induced by YY1 knockdown, indicating involvement of EZH2 in the repressive complex recruited to the miR-31 region (Figures 4H and 4I; Figure S3H). These results collectively suggest that YY1 regulates PRC2 localization and initiates miR-31 suppression. Indeed, we found significant escalation of methylated histone H3K9 and H3K27 at the miR-31 locus of peripheral blood lymphocytes of ATL patients (Figure 4J), indicating that aberrant abundance of suppressive histone methylation may be responsible for the loss of miR-31 in the primary ATL cells.

Overexpression of PRC2 Components Leads to miR-31 Repression

Given that Polycomb-mediated repressiveness affects miR-31 level, our findings imply that the amount of EZH2 is related to miR-31 expression (Figure 4I; Figures S3G and S4A). We found a significantly upregulated expression of PRC2 components, especially EZH2 and SUZ12, in the primary ATL cells (Figures 5A and 5B; Table S3). Quantitative RT-PCR revealed that miR-31 levels inversely correlated with both *EZH2* and *SUZ12*, respectively (Figure 5C). miR-101 and miR-26a, which are putative negative regulators of EZH2, seem to be associated with this relationship in ATL cells (Figures S4B–S4E). To further confirm our hypothetical mechanism linking the epigenetic machinery and miR-31 expression, we performed a "loss-of-PRC2-function" assay. Retroviral delivery of shSUZ12 and shEZH2 in the ATL cell lines resulted in a great increase in the levels of *Pri-miR-31* and its mature form (Figure 5D; Figure S4F). Knockdown of PRC2 induced histone demethylation at H3K27 in the miR-31 region, which is concomitant with the decrease in H3K9me3 levels, EZH2 occupancy, and HDAC1 recruitment (Figure 5E), suggesting that this multimeric complex leads to a completely closed chromatin architecture as a result of histone modifications in the miR-31 genomic region.

To further examine whether the proposed mechanism holds true in other human cancers, we analyzed a couple of carcinoma cell lines, including HeLa cells and nonmetastatic and metastatic breast carcinoma cell lines, MCF7 and MDA-MB-453 cells, respectively. qRT-PCR revealed that expression of *EZH2* and *SUZ12* inversely correlated with miR-31 levels (Figure S4G).

(B) miR-31 restoration by retroviral vector inhibits *NIK* RNA accumulation in TL-Om1 cells. The results of *NIK* and mature miR-31 quantifications are shown (n = 3, mean ± SD).
(C) miR-31 or shNIK expression downregulates NIK protein expression and inhibits downstream pathway of noncanonical NF-κB in TL-Om1 cells.
(D) Reduced nuclear translocation of RelA and RelB proteins in miR-31- or shNIK-expressing TL-Om1 cells.
(E) miR-31-dependent downregulation of NF-κB activity in TL-Om1 cells examined by EMSA.
(F) NF-κB-luciferase reporter assays (n = 5, mean ± SD). FLAG-NIK plasmid was transiently introduced 48 hr prior to the assay.
(G) miR-31 level is relevant to proliferation of ATL cells. Cell proliferation curve of TL-Om1 cells were evaluated in two FCS conditions (n = 3, mean ± SD).
(H) Apoptosis-related gene expression in TL-Om1 cells analyzed by qRT-PCR (n = 3, mean ± SD) and western blots.
(I) Lentivirus-mediated NIK depletion promotes basal and Fas antibody-mediated apoptosis. Venus-positive population represented lentivirus-infected cells. Apoptotic cells were determined by PE-Annexin V / 7-AAD stainings (n = 4). Representative FACS analyses are shown.
(J) miR-31 activates Caspase 3/7 determined by FACS (n = 3).
(K) miR-31 expression and NIK depletion induce tumor cell death. Primary tumor cell from ATL patient and healthy CD3+ T cells were infected with lentivirus and analyzed by FACS. The apoptotic cells were defined by sequential gating beginning with FSC-SSC to select intact lymphocytes, subgating on the Venus-positive population, and calculating the PE-Annexin V and 7-AAD profilings. Representative result is shown and summarized data are presented in Figure 6J. See also Figure S2.

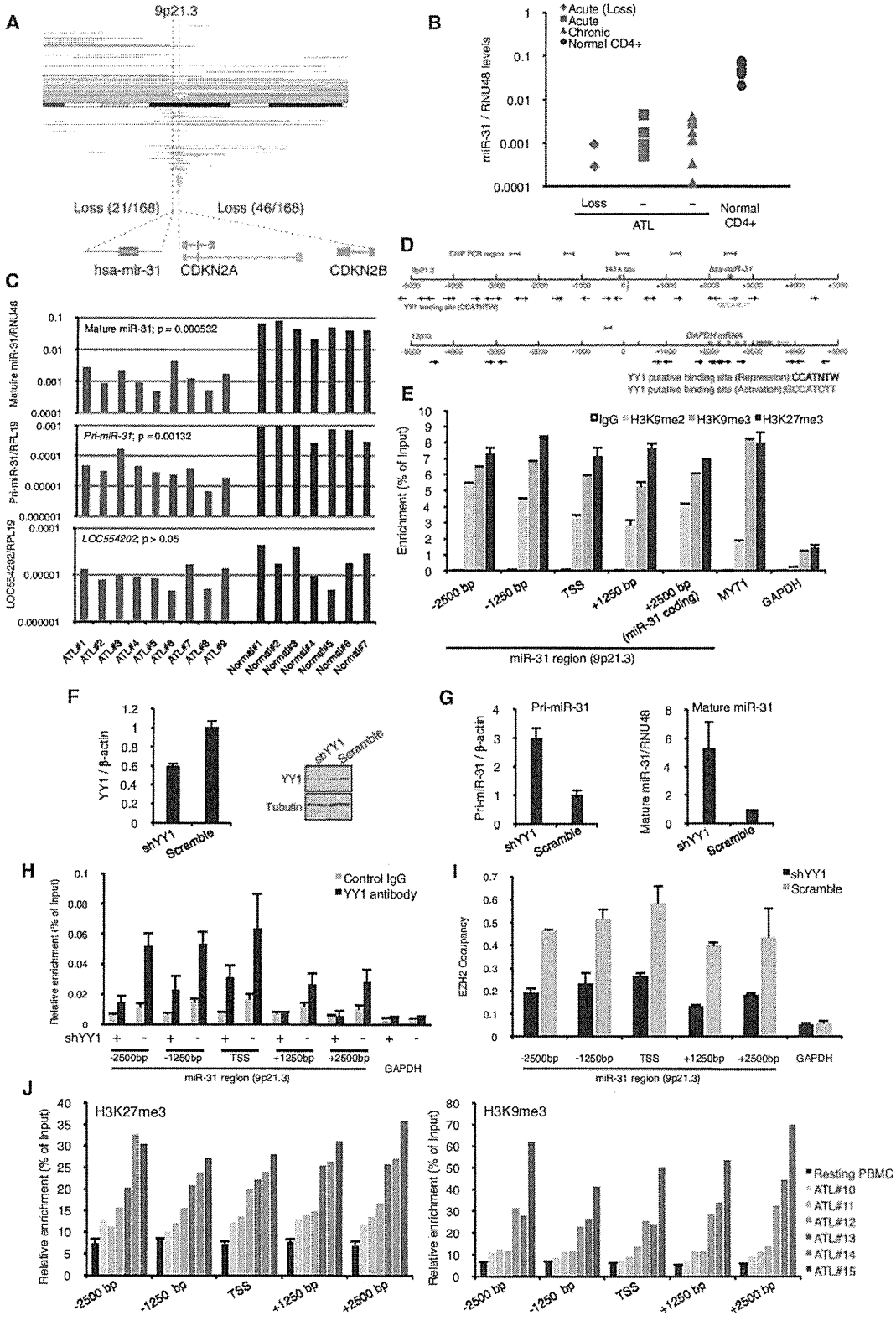
A
9p21.3
Loss (21/168)
Loss (46/168)
hsa-mir-31
CDKN2A
CDKN2B
B
Acute (Loss)
Acute
Chronic
Normal CD4+
miR-31 / RNU48 levels
Loss
ATL
Normal CD4+
C
Mature miR-31; p = 0.000532
Pri-miR-31; p = 0.00132
LOC554202; p > 0.05
Mature miR-31/RNU48
Pri-miR-31/RPL19
LOC554202/RPL19
ATL#1 ATL#2 ATL#3 ATL#4 ATL#5 ATL#6 ATL#7 ATL#8 ATL#9
Normal#1 Normal#2 Normal#3 Normal#4 Normal#5 Normal#6 Normal#7
D
YY1 putative binding site (Repression):CCATNTW
YY1 putative binding site (Activation):GCCATCTT
E
IgG H3K9me2 H3K9me3 H3K27me3
Enrichment (% of Input)
-2500 bp
-1250 bp
TSS
+1250 bp
+2500 bp (miR-31 coding)
MYT1
GAPDH
miR-31 region (9p21.3)
F
YY1 / β-actin
shYY1
Scramble
YY1
Tubulin
G
Pri-miR-31
Pri-miR-31 / β-actin
Mature miR-31
Mature miR-31/RNU48
H
Control IgG
YY1 antibody
Relative enrichment (% of Input)
shYY1
-2500bp
-1250bp
TSS
+1250bp
+2500bp
GAPDH
miR-31 region (9p21.3)
I
shYY1
Scramble
EZH2 Occupancy
-2500bp
-1250bp
TSS
+1250bp
+2500bp
GAPDH
miR-31 region (9p21.3)
J
H3K27me3
H3K9me3
Relative enrichment (% of Input)
-2500 bp
-1250 bp
TSS
+1250 bp
+2500 bp
Resting PBMC
ATL#10
ATL#11
ATL#12
ATL#13
ATL#14
ATL#15

ChIP assays detected higher levels of trimethylated H3K27 and EZH2 occupancy in cells showing lower expression levels of miR-31 (Figure S4H). Furthermore, knockdown of EZH2 or SUZ12 restored miR-31 transcription in MDA-MB-453 and MCF7 cells (Figures 5F and 5G; Figure S4K, respectively), which are consistent with the results obtained with ATL cells. These results indicate a link between Polycomb-mediated epigenetic regulation and miR-31 transcription in ATL and breast cancer cell lines.

Polycomb Group Regulates NF-κB Pathway by Controlling miR-31 Expression

Based on our findings, we considered an aspect of the biological communication between epigenetic silencing and the NF-κB pathway through miR-31 regulation. The microarray data sets showed positive correlations between PRC2 components and miR-31 target gene, *NIK* expression (Figure 6A). The results also suggested that these factors tend to show higher levels in the aggressive subtype (acute type) than in the indolent subtypes (chronic and smoldering types), implying that these genes may play important roles in the clinical phenotype and prognosis of ATL. To examine this notion, we performed PRC2 knockdown in ATL cell lines. Western blots of these cells demonstrated decreased levels of NIK, p52, and phospho-IκBα (Figure 6B; Figure S5A), suggesting suppression of both canonical and noncanonical NF-κB cascade and activity (Figure 6C; Figures S5B and S5C). These results are consistent with those of miR-31 overexpression (Figures 3C–3F). Then, we tested whether exogenous manipulation of miR-31 could restore the effect of PRC2 loss. Anti-miR-31 treatment rescued impaired NF-κB activity in PRC2-disrupted cells (Figure 6D). On the other hand, overexpression of EZH2 induced NF-κB activation, which was partially canceled by the introduction of miR-31 precursor (Figure 6E; Figure S5D). These results suggest that Polycomb-mediated miR-31 suppression leads to NF-κB activation. Indeed, knockdown of the PRC2 complex led to reduced levels of cell proliferation and greater sensitivity to serum deprivation in ATL cells (Figure 6F; Figure S5E). In addition, PRC2 disruption showed a reduction in cell migration (Figure S5F).

To gain further insight into this general network, we studied the functions of miR-31 and the PRC2 complex in breast cancer cell lines. NF-κB activity was downregulated by knockdown of PRC2 components in MDA-MB-453 cells (Figure 6G; Figures S5G and S5H), although no significant differences were observed in cell proliferation (data not shown). Repression of NF-κB activity induced by knockdown of PRC2 components was partially restored by treatment with a miR-31 inhibitor, suggesting that PRC2 knockdown-mediated relief of NF-κB repression is at least a part of the result of the miR-31 induction. In addition, knockdown of PRC2 components resulted in a reduced level of receptor-initiated accumulation of NIK in B cells (Figure 6H). Our findings indicate a common molecular mechanism comprising Polycomb-mediated epigenetic regulation, miR-31 expression and the NF-κB signaling pathway.

Regulation of NF-κB by Polycomb family may in turn control the cellular apoptosis responses. We found that lentivirus-mediated EZH2 knockdown led to increased apoptotic sensitivity in TL-Om1 cells (Figure 6I). Additional expression of NIK inhibited the cell death induced by EZH2 knockdown, suggesting the reciprocal relationship between Polycomb and NF-κB cascades. By using primary tumor cells from patient, we tested the killing effect induced by miR-31, NIK knockdown, and EZH2 knockdown (Figure 6J; Figures S5I and S5J). All tested samples showed strong death response, demonstrating that survival of ATL cells was closely associated with miR-31, NIK, and EZH2, all of which show deregulated expression in ATL cells.

By qRT-PCR we finally examined the expression levels of some genes involved in the noncanonical NF-κB pathway. As shown in Figure 6K, the results clearly demonstrated higher expression levels of positive regulators such as *NIK*, *CD40*, and *LTBR*, and lower expression levels of the negative regulators such as *BIRC2/3* (cIAP1/2), which are involved in proteasomal degradation of NIK (Zarnegar et al., 2008a). These observations are in line with a previous report on Multiple Myeloma cells (Annunziata et al., 2007). In addition to these data, we obtained convincing evidence for a molecular aspect of NIK accumulation in ATL cells. Polycomb-dependent epigenetic gene silencing may be associated with miR-31 loss, followed by NF-κB activation and other signaling pathways (Figure 7).

DISCUSSION

Constitutive activation of NF-κB contributes to abnormal proliferation and inhibition of apoptotic cell death in cancer cells,

Figure 4. Genetic and Epigenetic Abnormalities Cause miR-31 Loss in ATL Cells

(A) Genomic loss of chromosome 9p21.3 in primary ATL cells. Copy number analyses revealed tumor-associated deletion of miR-31 region (21/168) and *CDKN2* region (46/168). Recurrent genetic changes are depicted by horizontal lines based on CNAG output of the SNP array analysis.

(B) miR-31 expression in various sample sets. Expression levels were evaluated by real-time PCR.

Loss, samples with genomic loss of the miR-31 region; (–) samples without genomic loss of the miR-31 region.

(C) PCR-based miR-31 quantifications in primary ATL samples. ATL samples without genetic loss in miR-31 region (n = 9, Figure S3B), and normal CD4+ T cells (n = 7) were tested. p values (ATL versus normal) are shown.

(D) YY1 binding motif cluster around transcriptional start site (TSS) of miR-31 region. Arrows represent positions of the motifs. Regions of PCR amplification for ChIP assay are shown.

(E) Repression-associated histone methylation in miR-31 region determined by ChIP assay (n = 3, mean ± SD). The results of relative enrichment against input control are presented and distance from miR-31 TSS is described. *MYT1* and *GAPDH* promoters are as positive or negative controls, respectively.

(F–I) YY1-dependent EZH2 occupancy in miR-31 locus. (F) YY1 knockdown in TL-Om1 cells. qRT-PCR (left, n = 3, mean ± SD) and western blotting (right) showed decreased YY1 level. (G) YY1 knockdown led to both primary and mature miR-31 restoration in TL-Om1 cells (n = 3, mean ± SD). (H) YY1 occupancy in miR-31 region analyzed by ChIP (n = 3, mean ± SD). YY1 occupancy in miR-31 locus was reduced by YY1 knockdown. (I) EZH2 occupancy in miR-31 region analyzed by ChIP (n = 3, mean ± SD). YY1 knockdown inhibited EZH2 recruitment in miR-31 region.

(J) Aberrant accumulation of repression-associated histone methylations widely in miR-31 region of primary ATL cells. PBMCs freshly isolated from ATL patients (n = 6) were analyzed by ChIP assay. PBMC from healthy adults were used for normal controls. See also Figure S3.

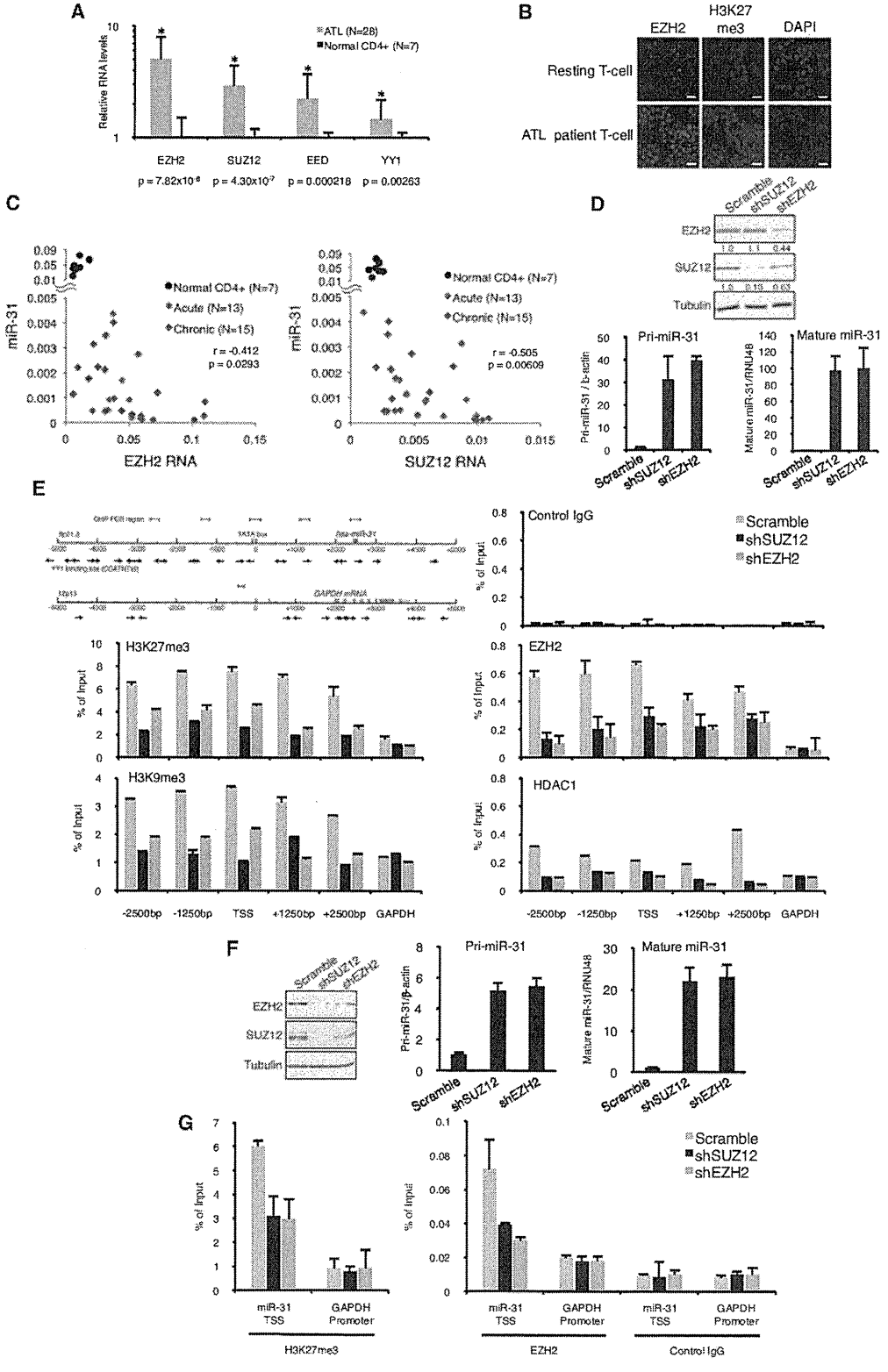
A
Relative RNA levels
ATL (N=28)
Normal CD4+ (N=7)
EZH2
SUZ12
EED
YY1
p = 7.82x10⁻⁸
p = 4.30x10⁻²
p = 0.000218
p = 0.00263
B
H3K27 me3
EZH2
DAPI
Resting T-cell
ATL patient T-cell
C
miR-31
Normal CD4+ (N=7)
Acute (N=13)
Chronic (N=15)
r = -0.412
p = 0.0293
EZH2 RNA
r = -0.505
p = 0.00609
SUZ12 RNA
D
Scramble
shSUZ12
shEZH2
EZH2
SUZ12
Tubulin
Pri-miR-31
Pri-miR-31 / b-actin
Mature miR-31
Mature miR-31/RNU48
E
Control IgG
Scramble
shSUZ12
shEZH2
% of Input
H3K27me3
EZH2
H3K9me3
HDAC1
-2500bp
-1250bp
TSS
+1250bp
+2500bp
GAPDH
F
Pri-miR-31
Mature miR-31
G
miR-31 TSS
GAPDH Promoter
H3K27me3
EZH2
Control IgG

including ATL, diffuse large B cell lymphoma (DLBCL), Hodgkin lymphoma, breast cancer, prostate cancer and others (Prasad et al., 2010). NF-κB is also essential for various cell functions, including inflammation, innate immunity, and lymphocytic development (Hayden and Ghosh, 2008). Identification of NF-κB determinants will lead to marked progress in understanding molecular pathology.

Our global analyses demonstrated an interesting miRNA expression signature as well as an aberrant mRNA expression profile, which may be associated with leukemogenesis in the primary ATL cells (Figures 1 and 6A). We revealed downregulation of tumor-suppressive miRNA including Let-7 family, miR-125b, and miR-146b, which can contribute to aberrant tumor cell signaling. Recent studies have suggested unique expression profiles of miRNAs in ATL (Yeung et al., 2008; Bellon et al., 2009), but loss of miR-31 has not been focused. Cellular amount of miRNAs may be susceptible to various environments such as transcriptional activity, maturation processing, and also epigenetic regulation. The end results appear to be affected by methodology employed and conditions and types of samples used. Our integrated expression profiling of primary ATL cells are based on a significantly larger number of samples and fruitfully provides intriguing information that may be useful in improving the understanding of T cell biology as well as in the identification of biomarkers for diagnosis.

Pleiotropy of miR-31 was first reported by Valastyan et al. (2009). The authors elegantly demonstrated the function of miR-31 in vivo and also identified several target genes that contribute to cell migration and invasiveness. In the present study, we focused on the functional significance of miR-31 in the regulation of NF-κB signaling that contributes to tumor cell survival.

Overexpression of NIK acts as an oncogenic driver in various cancers. In the present study, NIK was identified as a miR-31 target based on several lines of evidence. First, luciferase-3′ UTR reporter assay showed that *NIK* 3′ UTR sequence has a role for negative regulation (Figure S1B). By combining a specific inhibitor and mutations in miR-31-binding site, we demonstrated that miR-31 recognizes and negatively regulates the *NIK* 3′ UTR (Figures 2A and 2D). Second, by introducing a miR-31 precursor or inhibitor, we showed that amount of miR-31 inversely correlates with levels of NIK expression and downstream signaling (Figures 2E–2K). Third, genetic evidence indicated strong base pairing and biological conservation (Bartel, 2009) (Figures S1L–S1O). Our experimental approach illustrated that mmu-miR-31 regulates mouse *Map3k14* gene. Fourth, individual assessments using gene expression data clearly revealed an inverse correlation between the expression levels of miR-31 and *NIK* (Figure 3A). Collectively, we provide definitive evidence for the notion that miR-31 negatively regulates NIK expression and activity.

It is well known that the NIK level directly regulates NF-κB activity in various cell types (Thu and Richmond, 2010). We experimentally showed that miR-31 regulates noncanonical NF-κB activation stimulated by BAFF and CD40L, both of which are major B cell activating cytokines. Since signals from receptors are essential for the development and activity of B cells, the negative role of miR-31 in cytokines-induced NIK accumulation appears to be widely important in the noncanonical regulation of NF-κB in B cells and other cell types (Figures 2H–2K). Again, our findings revealed the role of NIK in the regulation of canonical NF-κB pathway. Strict regulation of NIK appears to be closely associated with the fate of lymphocytes.

The level of miR-31 was drastically suppressed in all tested primary ATL cells, and its magnitude is greater than that which has been reported in other cancers. Our results demonstrated a profound downregulation of miR-31 (fold change, 0.00403; Figure 1B) in all ATL cases, suggesting that miR-31 loss is a prerequisite for ATL development. Restoration of miR-31-repressed NF-κB activity in ATL cells, resulting in impairment of the proliferative index and apoptosis resistance (Figure 3). Furthermore, our results demonstrate that inhibition of NF-κB promotes tumor cell death in cell lines and also primary tumor cells from ATL patients (Figures 3 and 6), which are consistent with our previous observation (Watanabe et al., 2005). Since it is highly possible that miR-31 and relevant factors are pivotal in cancers, their expressions would have a great importance in view of biomarkers for the aberrant signaling and clinical outcomes.

By studying clinical samples and in vitro and ex vivo models, we obtained several biologically interesting results. First, we identified the Polycomb protein complex as a strong suppressor of miR-31. Generally, the Polycomb group constitutes a multimeric complex that negatively controls a large number of genes involved in cellular development, reproduction, and stemness (Sparmann and van Lohuizen et al., 2006). However, the key molecules involved in cancer development, progression, and prognosis are not yet fully understood. In breast and prostate cancers, oncogenic functions of EZH2 and NF-κB activation were reported independently (Kleer et al., 2003; Varambally et al., 2002; Suh and Rabson, 2004). Interestingly, these tumors show low miR-31 levels (Valastyan et al., 2009; Schaefer et al., 2010). Recently, Min et al. (2010) reported that EZH2 activates NF-κB by silencing the DAB2IP gene in prostate cancer cells.

Figure 5. Amount of PRC2 Components Epigenetically Links to miR-31 Expression in T Cells and Epithelial Cells

(A) Overexpression of PRC2 components in primary ATL cells measured by qRT-PCR (ATL, n = 28; normal, n = 7; mean ± SD). These results were supported by the data of gene expression microarray (Table S3).

(B) Escalation of EZH2 protein and trimethylated H3K27 levels in primary ATL cells illustrated by immunocytostaining (n = 4, a representative result is shown). Resting T cells were as normal control. Scale bars = 20 μm.

(C) Statistical correlation among the levels of miR-31, *EZH2*, and *SUZ12* in individual ATL samples. Correlation coefficients within ATL samples are shown in the graphs.

(D and E) Loss of PCR2 function causes chromatin rearrangement and miR-31 upregulation. (D) TL-Om1 cells expressing shSUZ12, shEZH2, and scrambled RNA were established by retroviral vector. The levels of EZH2, SUZ12, *Pri-miR-31*, and mature miR-31 were measured by western blotting and qRT-PCR (n = 3, mean ± SD). (E) Results of ChIP assays with indicated antibodies (n = 3, mean ± SD). Amounts of immunoprecipitated DNA were analyzed by region-specific PCR. *GAPDH* promoter served as a region control.

(F and G) Knockdown of Polycomb family proteins in MDA-MB-453 cells. (F) EZH2 and SUZ12 are shown by western blot. miR-31 level was examined by qRT-PCR (n = 3, mean ± SD). (G) Histone methylation and EZH2 occupancy evaluated by ChIP assay (n = 3, mean ± SD). See also Table S3 and Figure S4.

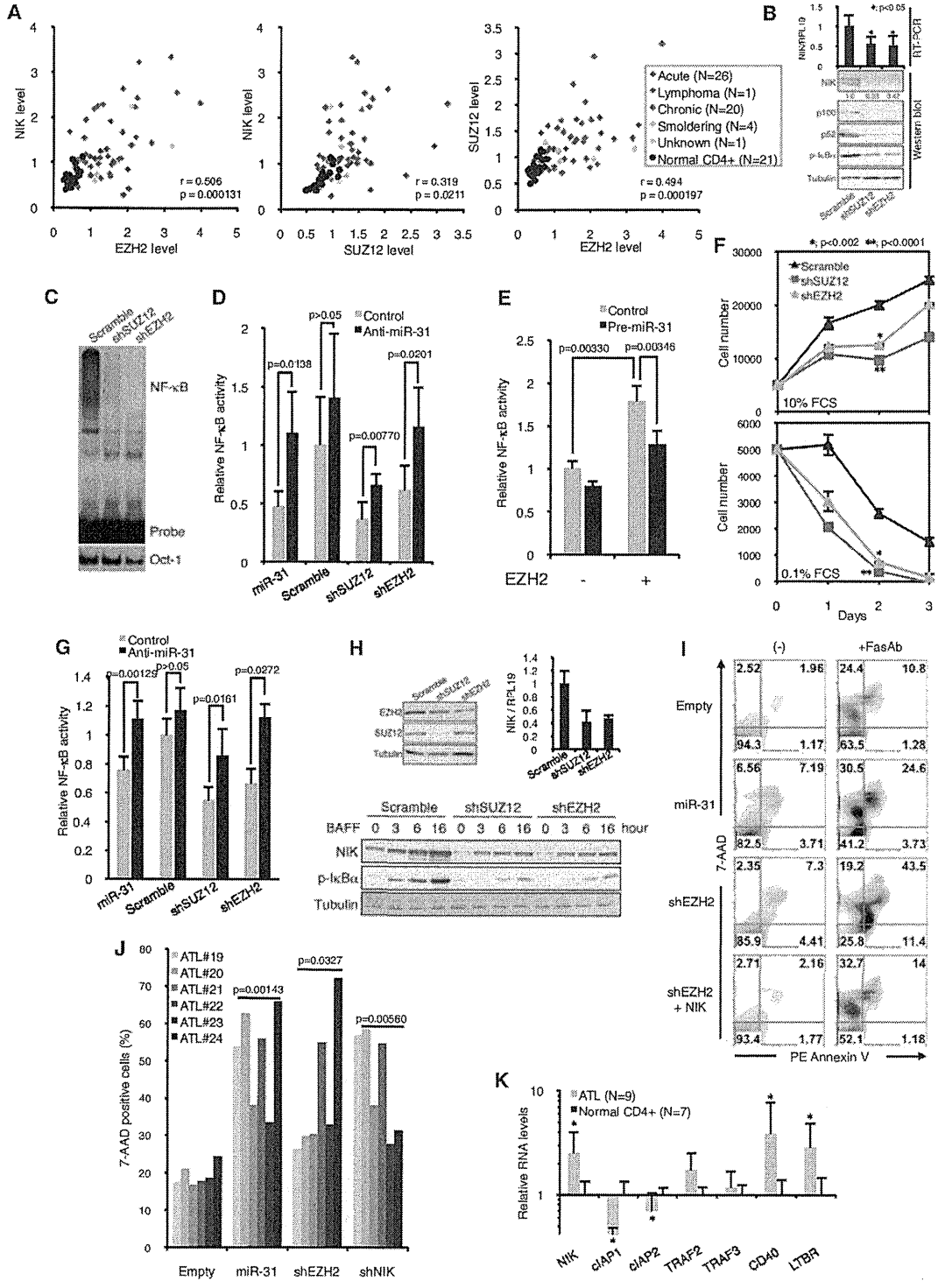

Figure 6. Epigenetic Change Driven by Polycomb Group Mediates NF-κB Signaling through miR-31 Regulation

(A) Reciprocal relationship of mRNA expression between *NIK* and Polycomb group in primary samples. Pearson's correlation coefficients among ATL samples are shown.

(B) PRC2 knockdown negatively affects NF-κB signaling in TL-Om1 cells. After establishment of PRC2 knockdown, the levels of *NIK* RNA (n = 4, mean ± SD) and proteins of NIK, p52/p100, and phospho-IκBα were examined.

(C) Downregulation of NF-κB activity in PRC2-disrupted cells detected by EMSA.

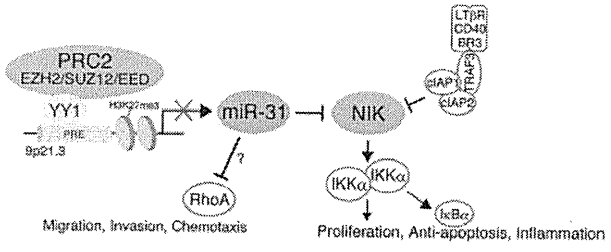

Figure 7. Proposed Model for ATL and Other Tumor Cells
Polycomb repressive factors are linked to NIK-dependent NF-κB activation via miR-31 regulation.

In the present study, we found that the Polycomb group regulates miR-31 expression and that elevated expression of EZH2 leads to NF-κB activation via NIK-miR-31 regulation in ATL and breast cancer cells (Figure 6). We also showed that restoration of miR-31 partially impaired Polycomb-mediated NF-κB operation (Figures 6D, 6E, and 6G), suggesting that miR-31 is involved in this relationship. Furthermore, a connection between NIK and PRC2 was observed in B cells (Figure 6H). Polycomb group proteins are essential in lymphocyte development and activation (Su et al., 2003, 2005). Further, given the NF-κB is a pivotal transcription regulator in normal and oncogenic functions, practical participations of epigenetic regulators and miR-31 in NF-κB signaling will increase our understanding of the molecular mechanisms of T cell functions. For generalization of the molecular axis in other cancers and normal cells, further study will be needed.

Second, YY1 is a recruiter of PRC2 to the miR-31 region. In humans, the Polycomb response element (PRE) has not been precisely identified. A good candidate for a mammalian recruiter of PRC2 is YY1, the homolog of *D. melanogaster* PHO (Simon and Kingston, 2009). We found an assembly of the YY1 binding motif in the miR-31 locus and demonstrated that YY1 knockdown dislodged EZH2 in this region (Figure 4I), which supports previous findings (Caretti et al., 2004). The detailed mechanism by which YY1 mediates recruitment of the Polycomb family may be important in the context of epigenetic regulation of orchestrated gene expression and T cell functions.

Third, Polycomb family proteins can control miRNA expression in an epigenetic fashion. The amount of PRC2 factors strongly influenced the degree of suppression of miR-31 expression (Figure 5). We speculate that, in addition to controlling the transcription, the Polycomb group can modulate translation via miRNA regulation. Furthermore, miR-101 and miR-26a are known to regulate EZH2 expression (Sander et al., 2008; Varambally et al., 2008), which is supported by our observation (Figure S4C). This signaling circuit will permit multiple gene regulation. Whereas genetic loss at the miR-31 locus is observed in some cases of ATL (Figure 4A), no genetic deletion in the miR-101-1 or miR-101-2 region was detected in ATL, which is not consistent with a previous finding in prostate cancer. Our results also suggested putative association between Let-7 family and EZH2 (Figure S4). Aberrant downregulations of these miRNAs in the primary ATL cells will be the next important questions to be addressed in efforts to improve understanding of the oncogenic signaling network.

By collaborative profiling of miRNA and mRNA expression, we identified a notable relationship between ATL subtypes and a gene cluster that contains miR-31, NIK, EZH2, and SUZ12. This finding suggests that an aberrant gene expression pattern correlates with the malignant phenotype, and this provides important clues about clinical manifestations and may help identify therapeutic targets against ATL cells (Figure 6A). Although HDAC inhibitors did not show effective responses (Figures S4I and S4J), emerging epigenetic drug such an EZH2 inhibitor (Fiskus et al., 2009) may pave a pathway leading to cures for various malignancies that involve constitutive activation of NF-κB.

In summary, we show that genetic and epigenetic loss of miR-31 is responsible for oncogenic NF-κB activation and malignant phenotypes in ATL. This provides evidence for the idea that miR-31 is an important tumor suppressor. An emerging pathway involving an epigenetic process, miR-31, and NF-κB will provide a conceptual advance in epigenetic reprogramming, inflammatory signaling, and oncogenic addiction.

EXPERIMENTAL PROCEDURES

Cell Lines and Primary ATL Cells

The primary peripheral blood mononuclear cells (PBMCs) from ATL patients and healthy volunteers used in the present work were a part of those collected with an informed consent as a collaborative project of the Joint Study on Prognostic Factors of ATL Development (JSPFAD). The project was approved by the Institute of Medical Sciences, the University of Tokyo (IMSUT) Human Genome Research Ethics Committee. Additional ATL clinical samples for copy number analysis were provided by Drs. Y. Yamada, Nagasaki University,

(D) NF-κB activity evaluated by reporter assays in the presence or absence of miR-31 inhibitor (n = 5, mean ± SD). Anti-miR-31 treatment partially rescued the NF-κB activity in PRC2 knockdowned TL-Om1 cells.
(E) Overexpressed EZH2 activates NF-κB via miR-31. Jurkat cells were transfected with an EZH2 plasmid together with miR-31 precursor or control RNA (n = 5, mean ± SD).
(F) PRC2 dysfunction changes TL-Om1 cell proliferation and response to serum starvation. Under conditions of 10% or 0.1% of FCS, cell growth curves were examined (n = 3, mean ± SD). PRC2 downregulation decreased cell growth with statistical significance.
(G) NF-κB activity in PRC2-knockdowned MDA-MB-453 cells in the presence or absence of miR-31 inhibitor were examined (n = 5, mean ± SD).
(H) PRC2 disruption inhibits BAFF-dependent NIK accumulation and IκBα phosphorylation in BJAB cells.
(I) Apoptotic cell death induced by lentivirus-mediated EZH2 knockdown in TL-Om1. Venus-positive populations were analyzed by Annexin V/7-AAD stainings (n = 3) and representative of FACS data are shown.
(J) Summary of primary tumor cell death. Lentivirus-based miR-31 expression, NIK knockdown, and EZH2 knockdown showed killing effects in six primary ATL samples. Statistical significances are shown in the graph. Results of FACS and qRT-PCR are shown in Figures S5I and S5J.
(K) Expression levels of genes involved in noncanonical NF-κB pathway in primary ATL cells (ATL, n = 9; normal, n = 7; mean ± SD). Relative expression levels were tested by qRT-PCR (*$p < 0.05$). See also Figure S5.

and K. Ohshima, Kurume University, where the projects were approved by the Research Ethics Committees of Nagasaki University and Kurume University, respectively. PBMC were isolated by Ficoll separation. ATL cells, primary lymphocytes, and all T cell lines were maintained in RPMI1640 supplemented with 10% of FCS and antibiotics. Clinical information of ATL samples is provided in Table S1.

Expression Analyses

Clinical samples for microarrays were collected by a collaborative study group, JSPFAD (Iwanaga et al., 2010). Gene expression microarray was used 4x44K Whole Human Genome Oligo Microarray (Agilent Technologies) and miRNA microarray was used Human miRNA microarray kit v2 (Agilent Technologies), respectively. Quantitative RT-PCR was performed with SYBRGreen (TAKARA). Mature miRNA assays were purchased from Applied Biosystems.

Copy Number Analyses

Genomic DNA from ATL patients was provided from the material bank of JSPFAD, Nagasaki University, and Kurume University, and was analyzed by Affymetrix GeneChip Human Mapping 250K Nsp Array (Affymetrix). Obtained data were analyzed by CNAG/AsCNAR program (Chen et al., 2008).

Oligonucleotides, Plasmids, and Retrovirus Vectors

All RT-PCR primers and oligonucleotides are described in Supplemental Experimental Procedures. miRNA precursor and inhibitor were from Applied Biosystems. Transfection of small RNA and other plasmid DNA were performed by Lipofectamine2000 (Invitrogen). For miRNA or shRNA expression, retroviral vectors (pSINsi-U6, TAKARA) were used.

3′ UTR-Conjugated miR-31 Reporter Assay

HeLa cells were cotransfected with 3′ UTR-inserted pMIR-REPORT firefly plasmid (Ambion), RSV-Renilla luciferase plasmid, and miRNA inhibitor. The cells were collected at 24 hr posttransfection, and Dual-luciferase reporter assay was performed (Promega).

Analysis of NF-κB Pathway

NF-κB activity was evaluated by EMSA and reporter assays as previously described (Horie et al., 2004). Antibodies for western blots are described in supplemental information. Cell proliferative assay was performed by Cell Counting Kit-8 (Dojindo).

Lentivirus Vectors and Apoptosis Analysis

A lentivirus vector (CS-H1-EVBsd) was provided from RIKEN, BRC, Japan. Lentivirus solution was produced by cotransfection with packaging plasmid (pCAG-HIVgp) and VSV-G- and Rev-expressing plasmid (pCMV-VSV-G-RSV-Rev) into 293FT cells. After infection of lentivirus, the apoptotic cell was evaluated by PE Annexin V / 7-AAD staining (BD PharMingen) and analyzed by FACS Calibur (Becton, Dickinson). Collected data were analyzed by FlowJo software (Tree Star).

ChIP Assay

ChIP assay was previously described (Yamagishi et al., 2009). Briefly, cells were crosslinked with 1% of formaldehyde, sonicated, and subjected to chromatin-conjugated IP using specific antibodies. Precipitated DNA was purified and analyzed by real-time PCR with specific primers (see Supplemental Experimental Procedures).

Computational Prediction

To identify miR-31 target genes, we integrated the output results of multiple prediction programs; TargetScan, PicTar, miRanda, and PITA. RNAhybrid was for secondary structure of miRNA-3′ UTR hybrid. TSSG program was for TATA box and TSS predictions. DNA methylation site was predicted by CpG island Searcher.

Statistical Analyses

Data were analyzed as follows: (1) Welch's t test for Gene Expression Microarray (p value cutoff at 10^{-6}) and miRNA Microarray (p value cutoff at 10^{-5}); (2) Pearson's correlation for two-dimensional hierarchical clustering analysis and individual assessment of microarray data sets; (3) two-tailed pared Student's t test with $p < 0.05$ considered statistically significant for in vitro cell lines and primary cells experiments, including luciferase assay, RT-PCR, ChIP assay, cell growth assay, and migration assay. Data are presented as mean ± SD.

ACCESSION NUMBERS

Coordinates have been deposited in Gene Expression Omnibus database with accession numbers, GSE31629 (miRNA microarray), GSE33615 (gene expression microarray), and GSE33602 (copy number analyses).

SUPPLEMENTAL INFORMATION

Supplemental Information includes three tables, five figures, and Supplemental Experimental Procedures and can be found with this article online at doi:10.1016/j.ccr.2011.12.015.

ACKNOWLEDGMENTS

We thank Dr. M. Iwanaga, Mr. M. Nakashima, and Ms. T. Akashi for support and maintenance of JSPFAD. We thank Drs. H. Miyoshi and A. Miyawaki for providing the Venus-encoding lentivirus vectors. We also thank Dr. R. Horie for experimental advices, and Drs. T. Kanno and T. Ishida for providing the MDA-MB-453. Grant support: Grants-in-Aid for Scientific Research from Ministry of Education, Culture, Sports, Science, and Technology of Japan to T.W. (No. 23390250) and by Grants-in-Aid from the Ministry of Health, Labour and Welfare to T.W. (H21-G-002 and H22-AIDS-I-002).

Received: November 3, 2010
Revised: August 12, 2011
Accepted: December 19, 2011
Published: January 17, 2012

REFERENCES

Annunziata, C.M., Davis, R.E., Demchenko, Y., Bellamy, W., Gabrea, A., Zhan, F., Lenz, G., Hanamura, I., Wright, G., Xiao, W., et al. (2007). Frequent engagement of the classical and alternative NF-kappaB pathways by diverse genetic abnormalities in multiple myeloma. Cancer Cell *12*, 115–130.

Bartel, D.P. (2009). MicroRNAs: target recognition and regulatory functions. Cell *136*, 215–233.

Bellon, M., Lepelletier, Y., Hermine, O., and Nicot, C. (2009). Deregulation of microRNA involved in hematopoiesis and the immune response in HTLV-I adult T-cell leukemia. Blood *113*, 4914–4917.

Caretti, G., Di Padova, M., Micales, B., Lyons, G.E., and Sartorelli, V. (2004). The Polycomb Ezh2 methyltransferase regulates muscle gene expression and skeletal muscle differentiation. Genes Dev. *18*, 2627–2638.

Chen, Y., Takita, J., Choi, Y.L., Kato, M., Ohira, M., Sanada, M., Wang, L., Soda, M., Kikuchi, A., Igarashi, T., et al. (2008). Oncogenic mutations of ALK kinase in neuroblastoma. Nature *455*, 971–974.

Davis, B.N., Hilyard, A.C., Lagna, G., and Hata, A. (2008). SMAD proteins control DROSHA-mediated microRNA maturation. Nature *454*, 56–61.

Fiskus, W., Wang, Y., Sreekumar, A., Buckley, K.M., Shi, H., Jillella, A., Ustun, C., Rao, R., Fernandez, P., Chen, J., et al. (2009). Combined epigenetic therapy with the histone methyltransferase EZH2 inhibitor 3-deazaneplanocin A and the histone deacetylase inhibitor panobinostat against human AML cells. Blood *114*, 2733–2743.

Hayden, M.S., and Ghosh, S. (2008). Shared principles in NF-kappaB signaling. Cell *132*, 344–362.

Hironaka, N., Mochida, K., Mori, N., Maeda, M., Yamamoto, N., and Yamaoka, S. (2004). Tax-independent constitutive IkappaB kinase activation in adult T-cell leukemia cells. Neoplasia *6*, 266–278.

Horie, R., Watanabe, M., Ishida, T., Koiwa, T., Aizawa, S., Itoh, K., Higashihara, M., Kadin, M.E., and Watanabe, T. (2004). The NPM-ALK oncoprotein

abrogates CD30 signaling and constitutive NF-kappaB activation in anaplastic large cell lymphoma. Cancer Cell *5*, 353–364.

Iwanaga, M., Watanabe, T., Utsunomiya, A., Okayama, A., Uchimaru, K., Koh, K.R., Ogata, M., Kikuchi, H., Sagara, Y., Uozumi, K., et al; Joint Study on Predisposing Factors of ATL Development investigators. (2010). Human T-cell leukemia virus type I (HTLV-1) proviral load and disease progression in asymptomatic HTLV-1 carriers: a nationwide prospective study in Japan. Blood *116*, 1211–1219.

Kleer, C.G., Cao, Q., Varambally, S., Shen, R., Ota, I., Tomlins, S.A., Ghosh, D., Sewalt, R.G., Otte, A.P., Hayes, D.F., et al. (2003). EZH2 is a marker of aggressive breast cancer and promotes neoplastic transformation of breast epithelial cells. Proc. Natl. Acad. Sci. USA *100*, 11606–11611.

Liao, G., Zhang, M., Harhaj, E.W., and Sun, S.C. (2004). Regulation of the NF-kappaB-inducing kinase by tumor necrosis factor receptor-associated factor 3-induced degradation. J. Biol. Chem. *279*, 26243–26250.

Malinin, N.L., Boldin, M.P., Kovalenko, A.V., and Wallach, D. (1997). MAP3K-related kinase involved in NF-kappaB induction by TNF, CD95 and IL-1. Nature *385*, 540–544.

Min, J., Zaslavsky, A., Fedele, G., McLaughlin, S.K., Reczek, E.E., De Raedt, T., Guney, I., Strochlic, D.E., Macconaill, L.E., Beroukhim, R., et al. (2010). An oncogene-tumor suppressor cascade drives metastatic prostate cancer by coordinately activating Ras and nuclear factor-kappaB. Nat. Med. *16*, 286–294.

Prasad, S., Ravindran, J., and Aggarwal, B.B. (2010). NF-kappaB and cancer: how intimate is this relationship. Mol. Cell. Biochem. *336*, 25–37.

Ramakrishnan, P., Wang, W., and Wallach, D. (2004). Receptor-specific signaling for both the alternative and the canonical NF-kappaB activation pathways by NF-kappaB-inducing kinase. Immunity *21*, 477–489.

Saitoh, Y., Yamamoto, N., Dewan, M.Z., Sugimoto, H., Martinez Bruyn, V.J., Iwasaki, Y., Matsubara, K., Qi, X., Saitoh, T., Imoto, I., et al. (2008). Overexpressed NF-kappaB-inducing kinase contributes to the tumorigenesis of adult T-cell leukemia and Hodgkin Reed-Sternberg cells. Blood *111*, 5118–5129.

Sander, S., Bullinger, L., Klapproth, K., Fiedler, K., Kestler, H.A., Barth, T.F., Möller, P., Stilgenbauer, S., Pollack, J.R., and Wirth, T. (2008). MYC stimulates EZH2 expression by repression of its negative regulator miR-26a. Blood *112*, 4202–4212.

Schaefer, A., Jung, M., Mollenkopf, H.J., Wagner, I., Stephan, C., Jentzmik, F., Miller, K., Lein, M., Kristiansen, G., and Jung, K. (2010). Diagnostic and prognostic implications of microRNA profiling in prostate carcinoma. Int. J. Cancer *126*, 1166–1176.

Simon, J.A., and Kingston, R.E. (2009). Mechanisms of polycomb gene silencing: knowns and unknowns. Nat. Rev. Mol. Cell Biol. *10*, 697–708.

Sparmann, A., and van Lohuizen, M. (2006). Polycomb silencers control cell fate, development and cancer. Nat. Rev. Cancer *6*, 846–856.

Su, I.H., Basavaraj, A., Krutchinsky, A.N., Hobert, O., Ullrich, A., Chait, B.T., and Tarakhovsky, A. (2003). Ezh2 controls B cell development through histone H3 methylation and Igh rearrangement. Nat. Immunol. *4*, 124–131.

Su, I.H., Dobenecker, M.W., Dickinson, E., Oser, M., Basavaraj, A., Marqueron, R., Viale, A., Reinberg, D., Wülfing, C., and Tarakhovsky, A. (2005). Polycomb group protein ezh2 controls actin polymerization and cell signaling. Cell *121*, 425–436.

Suh, J., and Rabson, A.B. (2004). NF-kappaB activation in human prostate cancer: important mediator or epiphenomenon? J. Cell. Biochem. *91*, 100–117.

Thu, Y.M., and Richmond, A. (2010). NF-κB inducing kinase: a key regulator in the immune system and in cancer. Cytokine Growth Factor Rev. *21*, 213–226.

Trabucchi, M., Briata, P., Garcia-Mayoral, M., Haase, A.D., Filipowicz, W., Ramos, A., Gherzi, R., and Rosenfeld, M.G. (2009). The RNA-binding protein KSRP promotes the biogenesis of a subset of microRNAs. Nature *459*, 1010–1014.

Valastyan, S., Reinhardt, F., Benaich, N., Calogrias, D., Szász, A.M., Wang, Z.C., Brock, J.E., Richardson, A.L., and Weinberg, R.A. (2009). A pleiotropically acting microRNA, miR-31, inhibits breast cancer metastasis. Cell *137*, 1032–1046.

Varambally, S., Dhanasekaran, S.M., Zhou, M., Barrette, T.R., Kumar-Sinha, C., Sanda, M.G., Ghosh, D., Pienta, K.J., Sewalt, R.G., Otte, A.P., et al. (2002). The polycomb group protein EZH2 is involved in progression of prostate cancer. Nature *419*, 624–629.

Varambally, S., Cao, Q., Mani, R.S., Shankar, S., Wang, X., Ateeq, B., Laxman, B., Cao, X., Jing, X., Ramnarayanan, K., et al. (2008). Genomic loss of microRNA-101 leads to overexpression of histone methyltransferase EZH2 in cancer. Science *322*, 1695–1699.

Ventura, A., and Jacks, T. (2009). MicroRNAs and cancer: short RNAs go a long way. Cell *136*, 586–591.

Watanabe, M., Ohsugi, T., Shoda, M., Ishida, T., Aizawa, S., Maruyama-Nagai, M., Utsunomiya, A., Koga, S., Yamada, Y., Kamihira, S., et al. (2005). Dual targeting of transformed and untransformed HTLV-1-infected T cells by DHMEQ, a potent and selective inhibitor of NF-kappaB, as a strategy for chemoprevention and therapy of adult T-cell leukemia. Blood *106*, 2462–2471.

Yamagishi, M., Ishida, T., Miyake, A., Cooper, D.A., Kelleher, A.D., Suzuki, K., and Watanabe, T. (2009). Retroviral delivery of promoter-targeted shRNA induces long-term silencing of HIV-1 transcription. Microbes Infect. *11*, 500–508.

Yamaguchi, K., and Watanabe, T. (2002). Human T lymphotropic virus type-I and adult T-cell leukemia in Japan. Int. J. Hematol. *76* (*Suppl 2*), 240–245.

Yeung, M.L., Yasunaga, J., Bennasser, Y., Dusetti, N., Harris, D., Ahmad, N., Matsuoka, M., and Jeang, K.T. (2008). Roles for microRNAs, miR-93 and miR-130b, and tumor protein 53-induced nuclear protein 1 tumor suppressor in cell growth dysregulation by human T-cell lymphotrophic virus 1. Cancer Res. *68*, 8976–8985.

Zarnegar, B.J., Wang, Y., Mahoney, D.J., Dempsey, P.W., Cheung, H.H., He, J., Shiba, T., Yang, X., Yeh, W.C., Mak, T.W., et al. (2008a). Noncanonical NF-kappaB activation requires coordinated assembly of a regulatory complex of the adaptors cIAP1, cIAP2, TRAF2 and TRAF3 and the kinase NIK. Nat. Immunol. *9*, 1371–1378.

Zarnegar, B.J., Yamazaki, S., He, J.Q., and Cheng, G. (2008b). Control of canonical NF-kappaB activation through the NIK-IKK complex pathway. Proc. Natl. Acad. Sci. USA *105*, 3503–3508.

Int J Hematol (2011) 94:430–434
DOI 10.1007/s12185-011-0934-4

Current status of HTLV-1 infection

Toshiki Watanabe

Received: 10 August 2011 / Revised: 31 August 2011 / Accepted: 2 September 2011 / Published online: 4 October 2011

Abstract It is 30 years since human T-cell leukemia virus type 1 (HTLV-1) was identified as the first human retrovirus. To assess the implications of the virus for human health it is very important to know the past and present prevalence. Most of the estimates of HTLV-1 prevalence are based on serological screening of blood donors, pregnant women and other selected population groups. The widely cited estimate that the number of HTLV-1 carriers in Japan is 1.2 million was calculated from data that are now more than 25 years old. Here I summarize previous reports of prevalence studies in the world and Japan. Then, a recent analysis of seroprevalence of healthy blood donors in Japan will be described in comparison with that of 1988. A decrease in the number of HTLV-1 carriers in Japan was demonstrated, however, it is still more than one million. The number has increased in the metropolitan areas, probably reflecting the migration of Japanese population. I conclude that there is a paucity of general population data in countries where HTLV-1 is endemic, and re-evaluation of HTLV-1 infection is required to understand the virus burden on the human health.

Keywords Seroprevalence of HTLV-1 · Vertical and horizontal transmission · Prevention of transmission

1 Introduction

Discovery of adult T-cell leukemia (ATL) by Takatsuki's group [1] was followed by the discovery of the first human retrovirus human T-cell leukemia virus (HTLV) and adult T-cell leukemia virus (ATLV) by research groups of the United State and Japan, respectively [2, 3]. In 1980, Poiesz et al. [2] identified HTLV in a T-cell line from a patient with cutaneous T-cell lymphoma. Independently of this, Hinuma and Miyoshi found specific antibodies against ATL cells in the patients' sera [3] and type C retrovirus particles produced by a T-cell line established from peripheral blood of ATL patient in 1981 [4]. In 1982, Yoshida et al. [5] identified ATLV as a human retrovirus. Soon, HTLV and ATLV were shown to be identical at the sequence level and were named HTLV type 1 (HTLV-1) [6, 7].

After the discovery of HTLV-1, related viruses have been isolated and HTLV is now composed of 4 related HTLVs, HTLV-1 to HTLV-4 [8]. However, only HTLV-1 has been convincingly linked to human diseases at present. HTLV-1 has six reported subtypes (subtypes A–F). Diverse studies have been performed on HTLV-1 subtyping but present a minor role in the epidemiological status of the virus. The great majority of infections are caused by the cosmopolitan subtype A, and there is no report of subtype influence on the pathogenic potential of HTLV-1 [9].

2 HTLV-1 infection in the world

Approximately 20 million people worldwide are estimated to be infected with HTLV-1 [10]. Among them, more than 90% remain asymptomatic carriers during their lives. Since 1986, HTLV-1 screening has been developed and was slowly implemented worldwide [11]. In 1993, HTLV-1 screening of blood donors was already performed in all developed countries and in many developing countries where HTLV-1 is endemic.

T. Watanabe (✉)
Department of Medical Genome Sciences,
Graduate School of Frontier Sciences, The University of Tokyo,
4-6-1 Shirokanedai, Minato-ku, Tokyo 108-8639, Japan
e-mail: tnabe@ims.u-tokyo.ac.jp

About the geographic distribution of the virus, a lot of studies have been done in these 30 years. Results indicate that Japan, Africa, the Caribbean islands, and Central and South America are the areas of highest prevalence in the world (reviewed in [12], [13]). However, the data from international prevalence studies should be interpreted and compared with caution as to the population selection criteria, because any difference in the diagnostic strategies can interfere with the final result. Data of the serological screening of healthy blood donors mainly provide basis for the estimation of the global prevalence of HTLV-1, which tends to underestimate the prevalence in the population. The geographic distribution of HTLV-1 infection is shown in Fig. 1 [13].

In addition to Japan, high rates of HTLV-1 infection have been reported for some Caribbean islands in studies of blood donors or segments of the general population. In Jamaica, the prevalence is around 5%. In Africa, the seroprevalence increases from the north to the south, varying from 0.6% in Morocco to greater than 5% in several sub-Saharan African countries, for example, Benin, Cameroon, and Guinea-Bissau, however, more studies are clearly required about these regions in detail. In Europe and North America, the prevalence is low and limited to groups that emigrated from endemic areas. For blood donors, very low rates were found in France (0.0039%) and the United States (0.025%). In South America, the virus was found in all countries, but more studies of the general population are needed to ascertain the real prevalence of HTLV-1. Medium prevalence was found in blood donors from Chile (0.73%) and Argentina (0.07%). In Australia, a prevalence of 14% was reported in a cluster among Aborigines in the Northern Territory, even though the prevalence in blood donors is low. The prevalence of HTLV-1 was highest in the two studies of Japanese islands (36.4%) and lowest in studies from Mongolia, Malaysia and India. In Haiti the prevalence was 3.8%; in Africa between 6.6 and 8.5% in Gabon, and 1.05% in Guinea. Only three studies were from West Africa and none were from the South; the only study from India was from the north of the country. It has to be

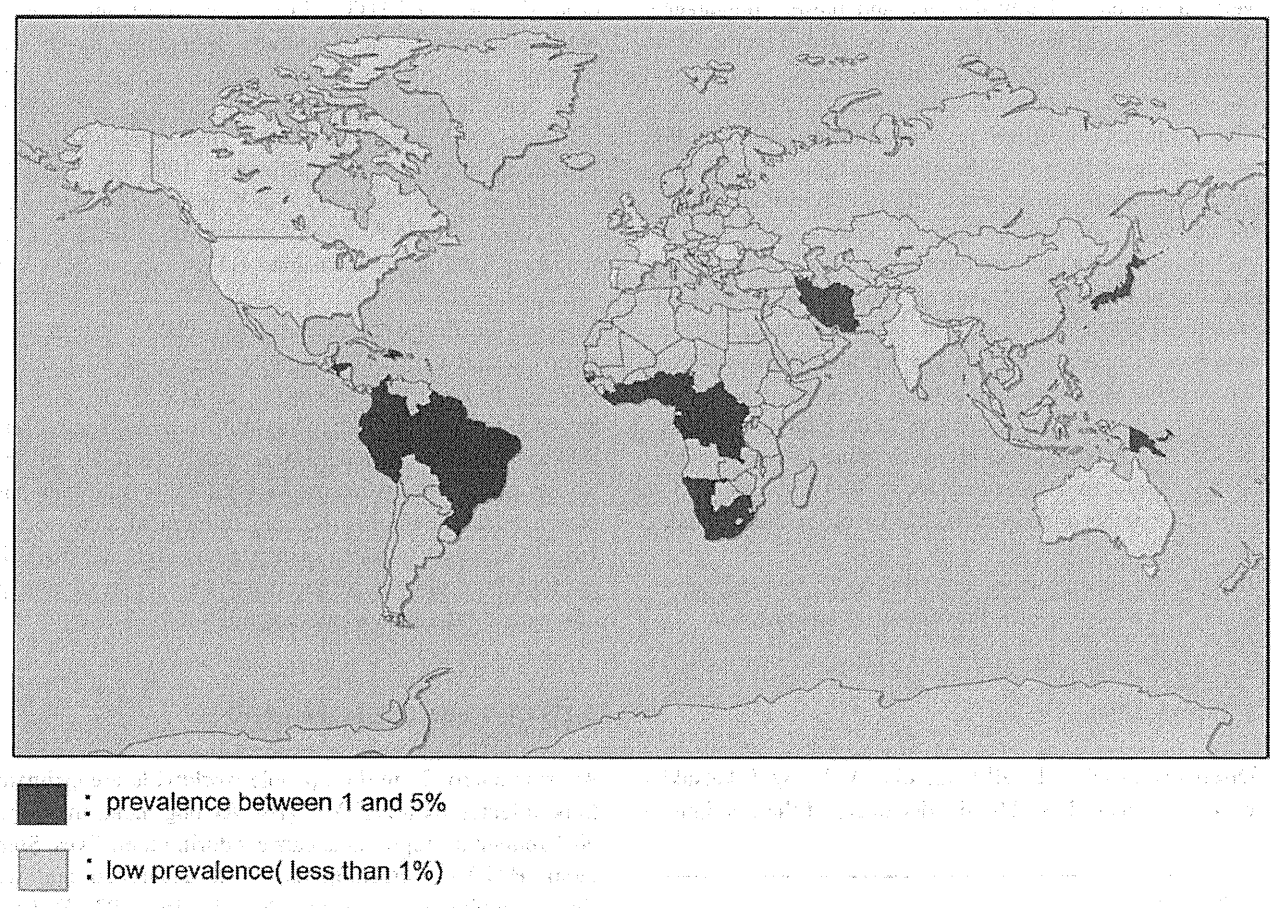

Fig. 1 Countries with endemic HTLV-I, defined as prevalence between 1 and 5% in some populations, are shown in *red*. Countries with reports of low prevalence (less than 1% in some groups), due mainly to immigration from endemic areas, are shown in *yellow*. It should be noted that HTLV-I endemic areas do not correspond exactly to the country boundaries shown in the map, for example, Brazil, Japan and Iran, where HTLV-I is limited to residents of certain areas of each country (modified from the reference [13])

concluded that there is a paucity of general population data from countries in which HTLV-1 is endemic, and that new studies are required to reevaluate the global burden of infection (reviewed in ref. [12] and [13]).

3 HTLV-1 Infection in Japan

3.1 Past studies of HTLV-1 carriers

Many efforts have been made to know the number of HTLV-1 carriers since the discovery of the virus in Japan. An example of early nationwide studies is the report of seropositive rates in the 15 blood centers of Japanese Red Cross [14]. It was reported that among 15 blood centers, 7 showed a higher positive rates between 6 and 30%, tested by indirect immunofluorescence assays (IFA). The other report is based on the data of all blood centers in Japan, which was the only study of all areas of Japan before the resent survey by Satake et al. [15]. They studied by IFA about 15,000 samples composed of 200 samples of blood donors aged from 40 to 64 from each center. The highest positive rate of 8% was observed in Kyushu area, and other areas showed positive rates of 0.3–1.2%. Based on these data, authors estimate seropositive rates of blood donors as about 3% in Kyushu and 0.08–0.3% in other areas of Japan. Using this study, Tajima et al., later estimated the total number of HTLV-1 carriers in Japan as 1.2 million [16].

There have been reports of community-based studies on seropositivities in Japan. One of the studies reported a very high seropositive rate (higher than 40%) in the people over 40 years of age [17]. An old study of the Tsushima Island revealed significant differences in the seropositive rate among villages with a high rate of more than 30% [18]. In Okinawa, a very high rate (21%) of HTLV-1 carriers in the general population of older than 40 was reported [19]. In a study of blood donors in Nagasaki prefecture from 1990 to 1999, positive rate of HTLV-1 antibodies decreased from 3.39 to 2.78% during 10 years. When focusing on the birth year of the donors, positive rates showed a decrease from 13.14 to 0.81% over the years from 1928 to 1983 [20]. On the other hand, the seroprevalence rate in Kumamoto prefecture was reported to be 3.6 or 4.7% in 1987–1988 [21, 22]. A survey on the general population was reported in Hokkaido. The average seropositive rate was 0.8% (male 0.6% and female 0.9%), with some regions showing higher seroprevalence rates as much as 5.2% [23].

Taken together, studies in 1980s and 1990s were mostly community-based ones using sera of blood donors. The oldest nationwide survey of the seroprevalence of HTLV-1 in blood donors and estimation of the number of HTLV-1 carriers [15, 16] had been referred to as the only published information until recently.

3.2 Recent studies of HTLV-1 infection in Japan

Based on the numbers of seropositive blood donors, Satake et al. have estimated the number of HTLV-1 carriers in Japan [15]. They analyzed data of blood donors who donated for the first time in 2006 and 2007, because Japanese Red Cross Blood center has notified the donors with the results of screening tests since 2000. This notification would have caused a bias in the population of total blood donors reducing the number of HTLV-1 carriers. In Satake's study, the total of number of tested was 1,196,321 (M: 704,074; F: 492,247), among them, HTLV-1 antibody was confirmed to be positive in 37,787 (M: 2,115; F: 1,672). Thus, the positive ratio was 0.32% for both male and female. Since the ages of blood donors were limited between 16 and 64, they estimated the seropositive rates of the peoples of younger than 15 or older than 65 by an assumption that the positive rate will increase exponentially in the young population, and for the aged people, by adding the average increase in the percentage in each age group in 20 years comparing with the data in 1988. Consequently, the estimated number of HTLV-1 carriers in 2007 was 1,078,722. The number of HTLV-1 carriers was estimated to be 492,582 in Kyushu area (including Okinawa), 171,843 in Kinki area (containing city areas of Osaka, Kyoto, Kobe) and 190,609 in Kanto area (containing the greater Tokyo area). The percentages of carriers in these areas among the total carriers were 45.7, 15.9 and 17.7%, respectively.

The age distribution of carriers showed a shift of the peak to the aged population. In 1988, the largest number of carriers was observed in the age group of 50–59, whereas in 2007 it was in the age groups of 60–69 and 70–79. The number of carriers in the age groups between 0–9 and 50–59 showed a significant decrease. This decline could be explained by changes in the life styles of Japanese people such as smaller number of children per family and shorter period of breast feeing. However, the exact reasons remain to be elucidated, especially considering the same tendency observed in the study of Brazilian people [24] and the age-dependent increase in the seropositivity in the colony of Japanese monkeys [25, 26].

Comparison of the regional distribution of the carriers in the present study with that reported by a Japanese study group in 1990 [27] revealed a significant decrease of the HTLV-1 carriers in Kyushu area (50.9 to 45.7%) and an increase in Kanto area (10.8 to 17.7%). The observed changes were considered to be mainly due to the migration of Japanese people from the Kyushu/Okinawa area to the metropolitan areas (Fig. 2). This interpretation is supported by the observation of Uchimaru et al. [28], who studied HTLV-1 carriers in Tokyo area and revealed that many of HTLV-1 carriers in Tokyo are either born in

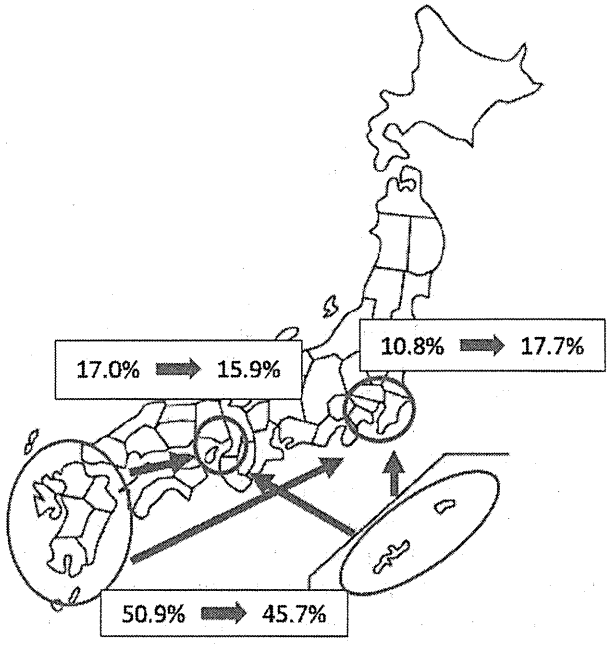

Fig. 2 Distribution of HTLV-1 carriers in Japan. Migration to the metropolitan areas is apparent. The number of HTLV-1 carriers in the endemic areas is still the largest, however, those in the great Tokyo area is significantly increasing

the endemic areas or the descendants of migrants from those areas.

4 Remaining problems and future directions

We have attributed the decrease in the HTLV-1 prevalence in Japan to the modernization and westernization of life styles of Japanese people. However, when we consider the same tendency in Brazil and age-dependent increase of seropositive rates in Japanese monkeys, we have to be cautious about interpretation of the observed data and may have to re-evaluate the meaning of the age-dependent carrier rates.

Another point that was raised by Satake's study is unexpectedly high increase in the positive rates in 20 years in the age-cohort [15]. This indicates the presence of horizontal transmission of the virus, probably through sexual contacts. This mode of infection should have contributed, at least to some extent, to the age-dependent increase in the positive rates. Thus, epidemiological studies on the horizontal transmission are definitely required; however, no such studies are now under way in Japan.

Taken together, we have to realize that we do not have enough data about the prevalence of HTLV-1 even in Japan, where serological data of blood donors are the only information to estimate the prevalence. Serological screening of the pregnant women that started in 2011 will provide valuable information about young females in Japan. Since the number of carriers who develop ATL is estimated about 1,200 per year in Japan, we have to expect more than 20,000 ATL patients from the present carriers in the future. In addition to the screening for the blood donors, prevention of mother-to-child infection by stopping breast feeding will greatly reduce the vertical transmission, nonetheless, there still remain other modalities of HTLV-1 infection, that are sexual transmission and possible trans-uterine infection. Neutralizing antibodies are often observed in carriers of HTLV-1 [29–32]. Furthermore, previous reports suggest that a primed immune response can be protective or prevent infection postviral exposure and challenge. It was shown that maternally acquired antibody protect infants from HTLV-1 infection in the early months of life [33]. A vaccine candidate based on an envelope expressing vaccinia virus provides protection to experimentally challenged primates [34, 35], and an attenuated viral strain provides long-term protection against the closely related bovine leukemia virus [36]. Taking all these into consideration, a costeffective vaccine may be a viable objective for prophylactic intervention in HTLV-1-endemic areas.

References

1. Uchiyama T, Yodoi J, Sagawa K, Takatsuki K, Uchino H. Adult T-cell leukemia: clinical and hematologic features of 16 cases. Blood. 1977;50:481–92.
2. Poiesz BJ, Ruscetti FW, Gazdar AF, Bunn PA, Minna JD, Gallo RC. Detection and isolation of type C retrovirus particles from fresh and cultured lymphocytes of a patient with cutaneous T-cell lymphoma. Proc Natl Acad Sci USA. 1980;77:7415–9.
3. Hinuma Y, Nagata K, Hanaoka M, Nakai M, Matsumoto T, Kinoshita KI, et al. Adult T-cell leukemia: antigen in an ATL cell line and detection of antibodies to the antigen in human sera. Proc Natl Acad Sci USA. 1981;78:6476–80.
4. Miyoshi I, Kubonishi I, Yoshimoto S, Akagi T, Ohtsuki Y, Shiraishi Y, et al. Type C virus particles in a cord T-cell line derived by co-cultivating normal human cord leukocytes and human leukaemic T cells. Nature. 1981;294:770–1.
5. Yoshida M, Miyoshi I, Hinuma Y. Isolation and characterization of retrovirus from cell lines of human adult T-cell leukemia and its implication in the disease. Proc Natl Acad Sci USA. 1982;79:2031–5.
6. Watanabe T, Seiki M, Yoshida M. Retrovirus terminology. Science. 1983;222:1178.
7. Gallo RC. History of the discoveries of the first human retroviruses: HTLV-1 and HTLV-2. Oncogene. 2005;24:5626–930.
8. Mahieux R, Gessain A. The human HTLV-3 and HTLV-4 retroviruses: new members of the HTLV family. Pathol Biol (Paris). 2009;57:161–6.
9. Ono A, Miura T, Araki S, Yamaguchi K, Takatsuki K, Mori S, et al. Subtype analysis of HTLV-1 in patients with HTLV-1 uveitis. Jpn J Cancer Res. 1994;85:767–70.

10. de Thé G, Kazanji M. An HTLV-I/II vaccine: from animal models to clinical trials? J Acquir Immune Defic Syndr Hum Retrovirol. 1996;13(Suppl 1):S191–8.
11. Inaba S, Sato H, Okochi K, Fukada K, Takakura F, Tokunaga K, et al. Prevention of transmission of human T lymphotropic virus type 1 (HTLV-1) through transfusion, by donor screening with antibody to the virus. One-year experience. Transfusion. 1989;29: 7–11.
12. Goncalves DU, Proietti FA, Ribas JGR, Araujo MG, Pinheiro SR, Guedes AC, et al. Epidemiology, treatment, and prevention of human T-cell leukemia virus type 1-associated diseases. Clin Microbiol Rev. 2010;23:577–89.
13. Proietti FA, Anna Bárbara, Carneiro-Proietti F, Bernadette C, Catalan-Soares, Murphy EL, et al. Global epidemiology of HTLV-I infection and associated diseases. Oncogene. 2005;24: 6058–68.
14. Hinuma Y, Komoda H, Chosa T, Kondo T, Kohakura M, Takenaka T, et al. Antibodies to adult T-cell leukemia-virus-associated antigen (ATLA) in sera from patients with ATL and controls in Japan: a nation-wide sero-epidemiologic study. Int J Cancer. 1982;29:631–5.
15. Satake M, Yamaguchi K. Annual report of the group study for survey of HTLV-1 infection and HTLV-1 related diseases in Japan. 2009 (in Japanese) (Manuscript submitted).
16. Tajima K. The 4th nation-wide study of adult T-cell leukemia/lymphoma (ATL) in Japan: estimates of risk of ATL and its geographical and clinical features. The T- and B-cell Malignancy Study Group. Int J Cancer. 1990;45:237–43.
17. Kohakura M, Nakada K, Yonahara M, Komoda H, Imai J, Hinuma Y. Seroepidemiology of the human retrovirus (HTLV/ATLV) in Okinawa where adult T-cell leukemia is highly endemic. Jpn J Cancer Res. 1986;77:21–3.
18. Tajima K, Kamura S, Ito S, Ito M, Nagatomo M, Kinoshita K, Ikeda S. Epidemiological features of HTLV-I carriers and incidence of ATL in an ATL-endemic island: a report of the community-based co-operative study in Tsushima, Japan. Int J Cancer. 1987;40:741–6.
19. Kohakura M, Nakada K, Yonahara M, Komoda H, Imai J, Hinuma Y. Seroepidemiology of the human retrovirus (HTLV/ATLV) in Okinawa where adult T-cell leukemia is highly endemic. Jpn J Cancer Res. 1986;77:21–3.
20. Chiyoda S, Kinoshita K, Egawa S, Inoue J, Watanabe K, Ifuku M. Decline in the positive rate of human T-lymphotropic virus type-1 (HTLV-1) antibodies among blood donors in Nagasaki. Intern Med. 2001;40:14–7.
21. Lee SY, Mastushita K, Machida J, Tajiri M, Yamaguchi K, Takatsuki K. Human T-cell leukemia virus type I infection in hemodialysis patients. Cancer. 1987;60:1474–8.
22. Iida S, Fujiyama S, Yoshida K, Morishita T, Shibata J, Sato T, et al. The seroprevalence of anti-HTLV-1 antibodies in patients with various liver diseases. Hepatogastroenterol. 1988;35:242–4.
23. Kwon KW, Yano M, Sekiguchi S, Iwanaga M, Fujiwara S, Oikawa O, et al. Prevalence of human T-cell leukemia virus type 1 (HTLV-I) in general inhabitants in non-adult T-cell leukemia (ATL)-endemic Hokkaido, Japan. In Vivo. 1994;8:1011–4.
24. Barcellos NT, Fuchs SC, Mondini LG, Murphy EL. Human T lymphotropic virus type I/II infection: prevalence and risk factors in individuals testing for HIV in counseling centers from Southern Brazil. Sex Transm Dis. 2006;33:302–6.
25. Ishida T, Yamamoto K, Kaneko R, Tokita E, Hinuma Y. Seroepidemiological study of antibodies to adult T-cell leukemia virus-associated antigen (ATLA) in free-ranging Japanese monkeys (Macaca fuscata). Microbiol Immunol. 1983;27:297–301.
26. Hayami M, Komuro A, Nozawa K, Shotake T, Ishikawa K, Yamamoto K, et al. Prevalence of antibody to adult T-cell leukemia virus-associated antigens (ATLA) in Japanese monkeys and other non-human primates. Int J Cancer. 1984;33:179–83.
27. Tajima K, Itoh S, Itoh T, Kinoshita K, Shimotohno K. Epidemiology of ATL and HTLV-1. In: the annual report of the group study "Inhibition of mother-to-child infection and ATL" (1990). 1991 (in Japanese).
28. Uchimaru K, Nakamura Y, Tojo A, Watanabe T, Yamaguchi K. Factors predisposing to HTLV-1 infection in residents of the greater Tokyo area. Int J Hematol. 2008;88:565–70.
29. Astier-Gin T, Portail JP, Londos-Gagliardi D, Moynet D, Blanchard S, Dalibart R, et al. Neutralizing activity and antibody reactivity toward immunogenic regions of the human T cell leukemia virus type I surface glycoprotein in sera of infected patients with different clinical states. J Infect Dis. 1997;175:716–9.
30. Londos-Gagliardi D, Armengaud MH, Freund F, Dalibart R, Moze E, Huet S, et al. Antibodies directed against a variable and neutralizable region of the HTLV-I envelope surface glycoprotein. Leukemia. 1997;11(Suppl. 3):38–41.
31. Hadlock KG, Rowe J, Perkins S, Bradshaw P, Song GY, Cheng C, et al. Neutralizing human monoclonal antibodies to conformational epitopes of human T-cell lymphotropic virus type 1 and 2 gp46. J Virol. 1997;71:5828–40.
32. Hadlock KG, Rowe J, Foung SK. The humoral immune response to human T-cell lymphotropic virus type 1 envelope glycoprotein gp46 is directed primarily against conformational epitopes. J Virol. 1999;73:1205–12.
33. Takahashi K, Takezaki T, Oki T, Kawakami K, Yahiski S, Fujiyoshi T, et al. Inhibitory effect of maternal antibody on mother-to-child transmission of human T-lymphotropic virus type I. Int J Cancer. 1991;49:673–7.
34. Kazanji M, Heraud JM, Merien F, Pique C, de The G, Gessain A, Jacobson S, et al. Chimeric peptide vaccine composed of B- and T-cell epitopes of human T-cell leukemia virus type 1 induces humoral and cellular immune responses and reduces the proviral load in immunized squirrel monkeys (*Saimiri sciureus*). J Gen Virol. 2006;87:1331–7.
35. Kazanji M, Tartaglia J, Franchini G, de Thoisy B, Talarmin A, Contamin H, Gessain A, de The G, et al. Immunogenicity and protective efficacy of recombinant human T-cell leukemia/lymphoma virus type 1 NYVAC and naked DNA vaccine candidates in squirrel monkeys (*Saimiri sciureus*). J Virol. 2001;75:5939–48.
36. Kerkhofs P, Gatot JS, Knapen K, Mammerickx M, Burny A, Portetelle D, Willems L, Kettmann R. Long-term protection against bovine leukaemia virus replication in cattle and sheep. J Gen Virol. 2000;81:957–63.

Bone Marrow Transplantation (2011) 46, 116–118

www.nature.com/bmt

ORIGINAL ARTICLE

Long-term outcomes after hematopoietic SCT for adult T-cell leukemia/lymphoma: results of prospective trials

I Choi[1], R Tanosaki[2], N Uike[1], A Utsunomiya[3], M Tomonaga[4], M Harada[5], T Yamanaka[6], M Kannagi[7] and J Okamura[6], on behalf of the ATLL allo-HSCT Study Group

[1]*Department of Hematology, National Kyushu Cancer Center, Fukuoka, Japan;* [2]*Stem Cell Transplantation Unit, National Cancer Center Hospital, Tokyo, Japan;* [3]*Department of Hematology, Imamura Bun-in Hospital, Kagoshima, Japan;* [4]*Molecular Medicine Unit, Department of Hematology, Atomic Bomb Disease Institute, School of Medicine, Nagasaki University, Nagasaki, Japan;* [5]*Kyushu University Graduate School of Medical Sciences, Fukuoka, Japan;* [6]*National Kyushu Cancer Center, Institute for Clinical Research, Fukuoka, Japan and* [7]*Medical Research Division, Department of Immunotherapeutics, Tokyo Medical and Dental University, Tokyo, Japan*

We have previously conducted clinical trials of allogeneic hematopoietic SCT with reduced-intensity conditioning regimen (RIC) for adult T-cell leukemia/lymphoma (ATLL)—a disease caused by human T-lymphotropic virus type 1 (HTLV-1) infection and having a dismal prognosis. Long-term follow-up studies of these trials revealed that 10 of the 29 patients have survived for a median of 82 months (range, 54–100 months) after RIC, indicating a possible curability of the disease by RIC. However, we have also observed that the patterns of post-RIC changes in HTLV-1 proviral load over time among the 10 survivors were classified into three patterns. This is the first report to clarify the long-term outcomes after RIC for ATLL patients.
Bone Marrow Transplantation (2011) **46,** 116–118; doi:10.1038/bmt.2010.92; published online 19 April 2010
Keywords: adult T-cell leukemia/lymphoma; allogeneic hematopoietic SCT; reduced-intensity conditioning regimen; HTLV-1 proviral load

Introduction

Adult T-cell leukemia/lymphoma (ATLL) is a peripheral T-cell malignancy that is caused by human T-lymphotropic virus type 1 (HTLV-1) infection and commonly affects individuals at an average age of 60 years. It has been reported that the 4-year survival rate was only 10.3%; in particular, patients with an acute or lymphoma subtype showed a dismal prognosis with a 4-year survival rate of approximately 5.0%.[1] Several retrospective studies for ATLL patients younger than 50 years have suggested the possible usefulness of allogeneic hematopoietic SCT (allo-HSCT) with a conventional conditioning chemotherapy regimen. However, the treatment-related mortality by conventional allo-HSCT was high (40–60%), probably due to the disease-specific immune deficiency at diagnosis.[2–4] This unacceptable level of mortality, even in the case of young patients, critically deters the applicability of conventional allo-HSCT for the general population of ATLL.

To permit the application of allo-HSCT for ATLL in patients aged more than 50 years, we can consider allo-HSCT for ATLL conditioned with reduced-intensity regimen (hereafter, allo-HSCT conditioned with reduced-intensity regimen is referred to as 'RIC'). Few retrospective studies have reported the results of RIC for ATLL so far; Shiratori *et al.*[5] followed up 15 patients after allo-HSCT (including 10 who received RIC) whose median age was 57 years and reported that the OS rate at 3 years reached 73%. Kato *et al.*[6] investigated the results of 33 patients with allo-HSCT from unrelated donors but this study included only 6 patients receiving RIC. However, our study group had previously activated the first clinical trials of RIC in 2001. These were two trials to clarify the feasibility of RIC: one studied RIC administered with immunosuppressant antithymocyte globulin (ATG) and the other studied RIC without ATG. The results have been already published elsewhere[7,8] and the treatment-related mortality in both trials collectively decreased to the 20% level, showing that RIC is a promising procedure for ATLL patients more than 50 years of age. In this report, we present the results of long-term follow-up of the two trials and discuss the longitudinal patterns of changes in HTLV-1 proviral load in survivors.

Patients and methods

The patient characteristics have been described in the previous reports.[7,8] Briefly, patients were eligible if they had ATLL of acute or lymphoma type and were aged between

Correspondence: Dr J Okamura, National Kyushu Cancer Center, Institute for Clinical Research, 3-1-1 Notame, Minami-ku, Fukuoka 811-1395, Japan.
E-mail: jyokamur@nk-cc.go.jp
Received 21 January 2010; revised 24 February 2010; accepted 3 March 2010; published online 19 April 2010

50 and 70 years. The patients were required to be in either CR or PR at the time of trial registration, and to have a HLA-identical sibling donor. The conditioning regimen consisted of fludarabine (30 mg/m^2 per day) for 5 days and BU (1 mg/kg orally per day) for 2 days. The patients in the first study also received low-dose ATG (2.5 mg/kg per day) for 2 days, whereas those in the second study did not. On day 0, G-CSF-mobilized peripheral blood grafts from their HLA-identical sibling donors were transplanted. To prevent GVHD, we continuously infused CYA (3 mg/kg per day) starting on day −1. The degree of donor–recipient chimerism in peripheral blood mononuclear cells was examined according to the previously reported method.[9] The HTLV-1 proviral load was estimated using blood samples obtained before and at 1, 2, 3, 6, 12 months and every year after transplantation. HTLV-1 proviral DNA was measured by the quantitative PCR amplification of HTLV-1 pX DNA.[10] The detection limit of the HTLV-1 proviral load was 0.5 copies per 1000 cells. The OS curve was estimated by the Kaplan–Meier method.

Results and discussion

Long-term survivors after RIC

In all, 15 and 14 patients were registered in the first and second studies, respectively. Eleven (six and five in the first and second studies, respectively) and eight (four in each study) patients died because of ATLL and the treatment, respectively. The last treatment-related death occurred 26 months after RIC. Characteristics of the remaining 10 patients (5 in each study) are summarized in Table 1. They are currently alive with a median follow-up period of 82 months after RIC (range, 54–100 months). Of the surviving patients, six and four patients had the acute and lymphoma types of ATLL. Of 10 patients, 5 received the grafts from HTLV-1-positive sibling donors. The OS rate at 60 months (5 years) was 34% (95% confidence interval, 18–51). No death was reported beyond 36 months after RIC (Figure 1).

Of the 10 survivors, 3 developed nonhematological relapse in the skin and/or lymph nodes within a half year after RIC (Table 1). However, remission was achieved again in these patients after the discontinuation of CYA, immunosuppressive agent, and the administration of additional treatments. In one of these patients, remission was achieved with the cessation of CYA alone. Two other patients were treated with systemic chemotherapy as well as local irradiation or donor lymphocyte infusion after the discontinuation of CYA, and thereafter obtained remission. These three patients survived for 100, 88 and 54 months after RIC, respectively. Because disease recurrence is usually fatal, the clinical course for the three patients was unique. It is suggested that the newly established immunological environment after RIC might have contributed to the eradication of ATLL lesions after early relapse.

All the 10 survivors developed acute GVHD (9 grades I–II and 1 grade III). Chronic GVHD was observed in all but one patient. Although immunosuppressive treatment was discontinued in 9 of the 10 patients, 1 patient is still receiving treatment due to active chronic GVHD. The development of chronic GVHD may suggest the presence of the graft-vs-ATLL effect. Of note is that 8 of 10 survivors received RIC when they were in PR after induction chemotherapy.

Kinetic patterns of HTLV-1 proviral load in long-term survivors

Serial changes in the HTLV-1 proviral load after RIC in the 10 long-term survivors are shown in Figure 2. The changes in the proviral load are heterogeneous but can be roughly classified into three patterns. In the first pattern, the proviral load became undetectable after RIC and continued to remain so; this pattern was seen in three patients. In the second pattern, the proviral load had become undetectable but returned to detectable levels thereafter; this pattern was also seen in three patients, all of whom had received RIC from HTLV-1-negative donors. Finally, in the third pattern, the proviral load had remained at the carrier level in four patients; these patients received the grafts from donors who were HTLV-1 carriers. All the 10 survivors continue to show complete donor chimera during the observation period regardless of the HTLV-1 proviral load level.

We noted that one survivor who was donated graft from an HTLV-1 carrier showed a strikingly high proviral load (nearly 1000 copies) during the first year after RIC; this

Table 1 Characteristics of long-term survivors

Age (years)	*Gender*	*ATL subtype*	*Donor status of HTLV-1*	*Status at RIC*	*Acute GVHD*	*Chronic GVHD*	*Relapse*	*Treatment after relapse*	*Current Karnofsky PS score (%)*	*Survival after RIC (months)*
62	Male	Acute	(+)	PR	I	Yes	Lynd, skin (day 28)	d/c CsA	>90	100
66	Female	Acute	(+)	PR	II	Yes	No		>90	98
51	Male	Acute	(−)	PR	II	Yes	No		>90	98
53	Male	Lymph	(−)	PR	II	Yes	No		>90	91
54	Male	Lymph	(−)	CR	II	Yes	Lynd (day 171)	d/c CsA, Rx, Cx	>90	88
55	Male	Lymph	(+)	PR	II	Yes	No		>90	75
62	Male	Acute	(+)	CR	II	Yes	No		>90	74
50	Female	Lymph	(−)	PR	I	Yes	No		>90	62
56	Male	Acute	(−)	PR	II	Yes	Skin (day 29)	d/c CsA, DLI, steroid	>90	54
53	Female	Acute	(+)	PR	III	No	No		>90	54

Abbreviations: Cx = chemotherapy; d/c = discontinued; DLI = donor lymphocyte infusion; lynd = lymph node; PS = performance status; RIC = hematopoietic stem cell transplantation conditioned with reduced-intensity regimen; Rx = radiation therapy.

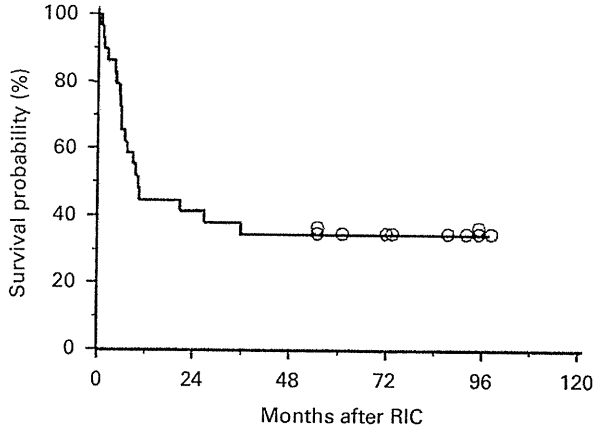

Figure 1 Kaplan–Meier curves for OS following RIC for ATLL. Circles show survivors (censored cases).

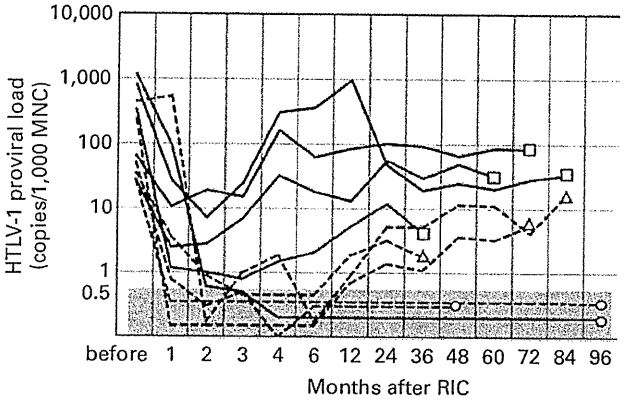

Figure 2 The longitudinal patterns of HTLV-1 proviral load after RIC in 10 long-term survivors. The HTLV-1 proviral load was measured by assaying serial blood samples after RIC by real-time PCR amplification of pX DNA and is expressed as copies per 1000 mononuclear cells (MNC). A load of less than 0.5 copies per 1000 MNC was considered undetectable, which is shown by the shaded area. A solid line indicates a patient who received a transplant from an HTLV-1 carrier donor whereas a dotted line indicates a patient from an HTLV-1-negative donor. Each circle, triangle or square indicates the latest measurement for the patient. Circle shows a pattern that the proviral load became undetectable after RIC and continued to remain so. Triangle shows a pattern that the proviral load had become undetectable but returned to detectable levels thereafter. Square shows a pattern that the proviral load had remained at the carrier level.

load then gradually decreased to the carrier level in the second year and the patient is currently surviving without any relapse. A temporary proliferation of HTLV-1-infected (nonleukemic) donor cells, as confirmed by a chimerism analysis, might have occurred due to some unknown etiology.

Conclusion

The long-term follow-up in our prospective studies has shown that one-third of the patients have survived and remain free of ATLL. We have also observed the different patterns of changes in proviral load; the pattern of changes in patients who received the grafts from HTLV-1-positive donors was different from that in patients who received the grafts from HTLV-1-negative donors. In conclusion, this is the first report on the long-term outcomes of ATLL patients who received allo-HSCT, and we have confirmed that RIC from matched sibling donors is a feasible treatment modality for ATLL, and that this treatment has a possible curative effect in patients with ATLL.

Conflict of interest

The authors declare no conflict of interest

References

1 Shimoyama M. Diagnostic criteria and classification of clinical subtypes of adult T-cell leukaemia-lymphoma. A report from the Lymphoma Study Group (1984–87). *Br J Haematol* 1991; **79**: 428–437.
2 Utsunomiya A, Miyazaki Y, Takatsuka Y, Hanada S, Uozumi K, Yashiki S *et al.* Improved outcome of adult T cell leukemia/lymphoma with allogeneic hematopoietic stem cell transplantation. *Bone Marrow Transplant* 2001; **27**: 15–20.
3 Kami M, Hamaki T, Miyakoshi S, Murashige N, Kanda Y, Tanosaki R *et al.* Allogeneic haematopoietic stem cell transplantation for the treatment of adult T-cell leukaemia/lymphoma. *Br J Haematol* 2003; **120**: 304–309.
4 Fukushima T, Miyazaki Y, Honda S, Kawano F, Moriuchi Y, Masuda M *et al.* Allogeneic hematopoietic stem cell transplantation provides sustained long-term survival for patients with adult T-cell leukemia/lymphoma. *Leukemia* 2005; **19**: 829–834.
5 Shiratori S, Yasumoto A, Tanaka J, Shigematsu A, Yamamoto S, Nishio M *et al.* A retrospective analysis of allogeneic hematopoietic stem cell transplantation for adult T cell leukemia/lymphoma (ATL): clinical impact of graft-versus-leukemia/lymphoma effect. *Biol Blood Marrow Transplant* 2008; **14**: 817–823.
6 Kato K, Kanda Y, Eto T, Muta T, Gondo H, Taniguchi S *et al.* Allogeneic bone marrow transplantation from unrelated human T-cell leukemia virus-I-negative donors for adult T-cell leukemia/lymphoma: retrospective analysis of data from the Japan Marrow Donor Program. *Biol Blood Marrow Transplant* 2007; **13**: 90–99.
7 Okamura J, Utsunomiya A, Tanosaki R, Uike N, Sonoda S, Kannagi M *et al.* Allogeneic stem-cell transplantation with reduced conditioning intensity as a novel immunotherapy and antiviral therapy for adult T-cell leukemia/lymphoma. *Blood* 2005; **105**: 4143–4145.
8 Tanosaki R, Uike N, Utsunomiya A, Saburi Y, Masuda M, Tomonaga M *et al.* Allogeneic hematopoietic stem cell transplantation using reduced-intensity conditioning for adult T cell leukemia/lymphoma: impact of antithymocyte globulin on clinical outcome. *Biol Blood Marrow Transplant* 2008; **14**: 702–708.
9 Thiede C, Florek M, Bornhauser M, Ritter M, Mohr B, Brendel C *et al.* Rapid quantification of mixed chimerism using multiplex amplification of short tandem repeat markers and fluorescence detection. *Bone Marrow Transplant* 1999; **23**: 1055–1060.
10 Sonoda J, Koriyama C, Yamamoto S, Kozako T, Li HC, Lema C *et al.* HTLV-1 provirus load in peripheral blood lymphocytes of HTLV-1 carriers is diminished by green tea drinking. *Cancer Sci* 2004; **95**: 596–601.

Cancer Science
The official journal of the Japanese Cancer Association JCA

Leukemic T cells are specifically enriched in a unique $CD3^{dim}CD7^{low}$ subpopulation of $CD4^+$ T cells in acute-type adult T-cell leukemia

Yamin Tian,[1,2] Seiichro Kobayashi,[1] Nobuhiro Ohno,[3] Masamichi Isobe,[3] Mayuko Tsuda,[3] Yuji Zaike,[4] Nobukazu Watanabe,[5] Kenzaburo Tani,[2] Arinobu Tojo[1,3] and Kaoru Uchimaru[3,6]

[1]Division of Molecular Therapy, Institute of Medical Science, The University of Tokyo, Tokyo; [2]Department of Molecular Genetics, Medical Institute of Bioregulation, Kyushu University, Fukuoka; [3]Department of Hematology/Oncology; [4]Clinical Laboratory, Research Hospital; [5]Laboratory of Diagnostic Medicine, Division of Stem Cell Therapy, Institute of Medical Science, The University of Tokyo, Tokyo, Japan

(Received July 27, 2010/Revised November 1, 2010/Accepted December 8, 2010/Accepted manuscript online December 14, 2010/Article first published online January 23, 2011)

The morphological discrimination of leukemic from non-leukemic T cells is often difficult in adult T-cell leukemia (ATL) as ATL cells show morphological diversity, with the exception of typical "flower cells." Because defects in the expression of CD3 as well as CD7 are common in ATL cells, we applied multi-color flow cytometry to detect a putative leukemia-specific cell population in the peripheral blood from ATL patients. $CD4^+CD14^-$ cells subjected to two-color analysis based on a CD3 *vs* CD7 plot clearly demonstrated the presence of a $CD3^{dim}CD7^{low}$ subpopulation in each of nine patients with acute-type ATL. The majority of sorted cells from this fraction showed a flower cell-like morphology and carried a high proviral load for the human T-cell leukemia virus type 1 (HTLV-I). Genomic integration site analysis (inverse long-range PCR) and analysis of the T cell receptor Vβ repertoire by flow cytometry indicated that the majority of leukemia cells were included in the $CD3^{dim}CD7^{low}$ subpopulation. These results suggest that leukemic T cells are specifically enriched in a unique $CD3^{dim}CD7^{low}$ subpopulation of $CD4^+$ T cells in acute-type ATL. (*Cancer Sci* 2011; 102: 569–577)

Adult T-cell leukemia (ATL) is a malignant disorder caused by human T-cell leukemia virus type 1 (HTLV-I)[1] and is characterized clinically by generalized lymphadenopathy, hepatosplenomegaly, skin lesions, hypercalcemia and a characteristic morphology termed "flower cells." Importantly, ATL is one of the most incurable lymphoid malignancies. This disease is endemic to several regions in the world, including sub-Saharan Africa, the Caribbean basin, South America and Japan, and 10–20 million people are estimated to be infected by this virus worldwide.[2,3]

Evaluation of the response after chemotherapy for ATL partly depends on the proportion of ATL cells in the peripheral blood. However, the morphological diversity of ATL cells may lead to inaccurate estimations. Accurate estimation of the chemotherapeutic effect is pivotal in clinical practice because ATL cells often become chemoresistant, even during chemotherapy. Methods to detect ATL cells with greater precision than morphological examination are therefore required.

Aberrant expression of cell-surface antigens in myeloid/lymphoid leukemia cells has been studied extensively.[4–6] Using fluorescence-activated cell sorting (FACS) analysis, gating cells with diminished CD45 expression in acute myeloid/lymphoid leukemia is widely used for purifying leukemia cells. However, in ATL there are only limited data regarding the identification of transformed leukemia cells by similar methods. Previous studies indicated that most ATL cells lack CD7 and exhibit diminished CD3 expression.[7–10] Although a study using CD3 gating by FACS analysis has indicated that ATL cells were distinguishable from normal lymphocytes as a $CD3^{low}$ population,[10] these cells were not well characterized as ATL cells.

In the present study, we focused on the enrichment of ATL cells by constructing CD3 *vs* CD7 plots from multi-color FACS. $CD3^{dim}CD7^{dim}$ and $CD3^{dim}CD7^{low}$ cells were extensively studied and compared with normal control samples. Taken together, our data suggest that ATL cells are purified in $CD3^{dim}CD7^{low}$ subpopulations. The purification of ATL cells by FACS may therefore allow monitoring of disease activity and yield insight into the biology of this disease.

Materials and Methods

Cell lines and patient samples. TL-Om1, a HTLV-I-infected cell line, was provided by Dr. Toshiki Watanabe (The University of Tokyo), and was cultured in RPMI 1640 medium containing 10% fetal bovine serum. Peripheral blood samples were collected from patients admitted to our hospital (Research Hospital, Institute of Medical Science, The University of Tokyo, Tokyo, Japan) during the period from August 2009 to April 2010 with written informed consent. All patients were diagnosed with acute-type ATL according to Shimoyama's criteria.[8] Blood samples were collected before treatment using the LSG15 protocol[11] or during the recovery phase between chemotherapy sessions. Samples collected from five healthy volunteers (median age, 45 years) were used as normal controls. The present study was approved by the institutional review board of our hospital.

Flow cytometry and cell sorting. Peripheral blood mononuclear cells (PBMC) were isolated from heparin-treated whole blood by density gradient centrifugation using Lymphoprep (Axis-Shield, Dundee, UK) and subsequently suspended in phosphate-buffered saline (PBS) containing 5% mouse serum (DAKO, Glostrup, Denmark) for prevention of nonspecific antibody binding. Cells were stained using a combination of phycoerythrin (PE)-CD7, PE-Cy7-CCR4, allophycocyanin (APC)-CD25, APC-Cy7-CD3, Pacific Blue-CD4 and Pacific Orange-CD14. Pacific Orange-CD14 was purchased from Caltag-Invitrogen (Carlsbad, CA, USA). All other antibodies were obtained from BD BioSciences (San Jose, CA, USA). Propidium iodide (PI; Sigma, St Louis, MO, USA) was added to the samples to stain dead cells immediately prior to FACS analysis. Cells were also stained with APC-FoxP3 (eBioscience, San Diego, CA, USA) using intracellular staining methods as previously described.[12] A TCR-Vβ repertoire kit (Beckman Coulter, Miami, FL, USA) was used for T-cell receptor (TCR) Vβ repertoire analysis according to the manufacturer's instructions.

[6]To whom correspondence should be addressed.
E-mail: uchimaru@ims.u-tokyo.ac.jp

doi: 10.1111/j.1349-7006.2010.01833.x

A BD FACS Aria (BD Immunocytometry Systems, San Jose, CA, USA) was used for all multi-color FACS analysis and cell sorting. Data were analyzed using FlowJo software (Treestar, San Carlos, CA, USA).

Quantification of HTLV-I proviral load by real-time quantitative polymerase chain reaction (PCR). The HTLV-I proviral load in PBMC was quantified by real-time quantitative polymerase chain reaction (PCR; TaqMan method) using the ABI Prism 7000 sequence detection system (Applied Biosystems, Foster City, CA, USA) as previously described.[13] Briefly, a total of 50 ng of genomic DNA was extracted from human PBMC using a QIAamp DNA blood Micro kit (Qiagen, Hilden, Germany). Triplicate samples of the DNA were amplified. Each PCR mixture containing a HTLV-I pX region-specific primer pair at 0.1 μM (forward primer 5′-CGGATACCCAGTCTACGTGTT-3′ and reverse primer 5′-CAGTAGGGCGTGACGATGTA-3′), FAM-labeled probe at 0.1 μM (5′- CTGTGTACAAGGC-GACTGGTGCC-3′) and 1× TaqMan Universal PCR master mix

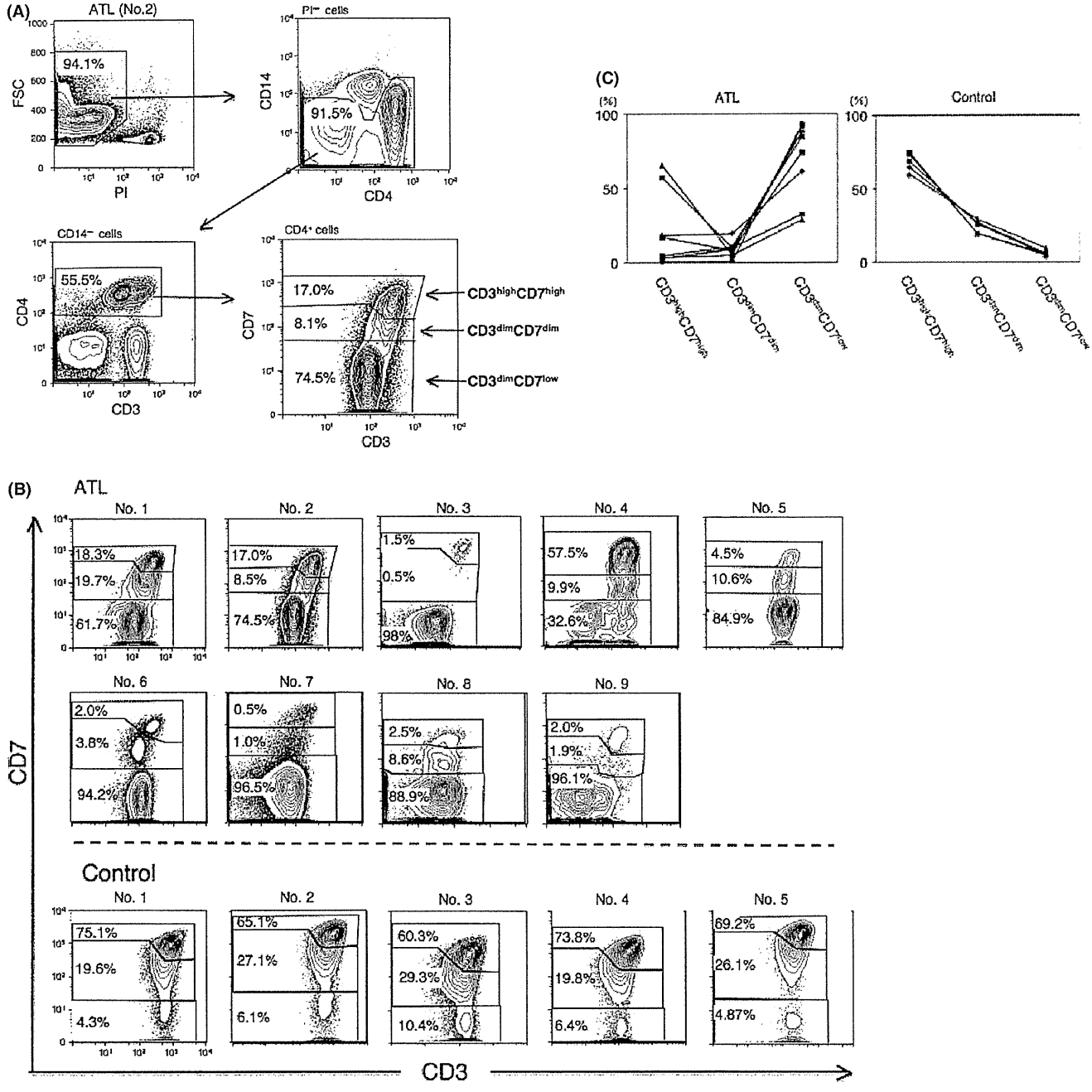

Fig. 1. CD3 *vs* CD7 plots from FACS analysis of patients with acute-type adult T-cell leukemia (ATL) and normal controls. (A) Representative flow cytometric analysis of a patient with acute-type ATL (patient no. 2). The CD3 *vs* CD7 plot in $CD4^+$ cells was constructed according to the gating procedure shown in this figure. In the plot, we designated three subpopulations: $CD3^{high}CD7^{high}$, $CD3^{dim}CD7^{dim}$ and $CD3^{dim}CD7^{low}$. (B) Flow cytometric profile of the CD3 *vs* CD7 plot in patients with acute-type ATL and normal controls. (C) Percentages of $CD3^{high}CD7^{high}$, $CD3^{dim}CD7^{dim}$ and $CD3^{dim}CD7^{low}$ subpopulations in $CD4^+$ T cells in patients with acute-type ATL and normal controls. Each line represents an individual sample. ATL group, $n = 9$; control group, $n = 5$; FSC, forward scatter; PI, Propidium iodide.

doi: 10.1111/j.1349-7006.2010.01833.x

Table 1. Clinical profile of nine acute-type ATL patients in the present study

No.	Age	Sex	WBC (/μL)	Lymph (%)	ATL cells† (%)	Organ involvement
1	60	M	5200	15.0	11.0	Skin
2	69	F	1600	43.5	9.0	Liver, LN, pleural effusion
3	61	M	18 620	24.7	43.7	Liver, uvea
4	59	F	6420	8.5	0.0	Liver, LN, skin
5	70	F	290	56.0	2.0	Liver, spleen, LN
6	60	F	4570	19.0	73.0	Skin
7	53	F	12 210	11.0	52.0	LN
8	74	F	6480	16.5	25.5	Liver, spleen, LN
9	63	F	34 810	21.5	33.5	Liver, spleen, LN, lung

†Proportion of ATL cells in the peripheral blood WBC evaluated by morphological examination. ATL, adult T-cell leukemia; LN, lymph nodes; Lymph, lymphocytes; WBC, white blood cells (normal range, 3500–9100/μL).

(Applied Biosystems) were subjected to 50 cycles of denaturation (95°C, 15 s) and annealing to extension (60°C, 1 min), following an initial Taq polymerase activation step (95°C, 10 min). The RNase P control reagent (Applied Biosystems) was used as an internal control for calculation of the input cell number (using VIC reporter dye). DNA extracted from TL-Om1 and normal human PBMC were used as positive and negative controls, respectively. The HTLV-I proviral load (%) was calculated as the copy number of the pX region per input cell number. To correct the deviation of acquired data in each experiment, data from TL-Om1 (positive control) were adjusted to 100% and the sample data was corrected by proportional calculation accordingly.

Inverse long PCR. For clonality analysis, inverse long PCR was performed. First, 1 μg of genomic DNA extracted from the FACS-sorted cells was digested with *Eco*RI, *Hin*dIII and *Pst*I at 37°C overnight. Purification of DNA fragments was performed using a QIAEX2 gel extraction kit (Qiagen). The purified DNA was self-ligated with T4 DNA ligase (Takara Bio, Otsu, Japan) at 16°C overnight. The circular DNA obtained from the *Eco*RI digestion fragment was then digested with *Mlu*I, which cuts the pX region of the HTLV-I genome and prevents amplification with the viral genome. Inverse long PCR was performed using Takara LA *Taq* polymerase (Takara Bio). The primer pairs for the *Eco*RI-treated template were: forward primer 5′-TGCCTGACCCTGCTTGCTCAACTCTACGTCTTTG-3′ and reverse primer 5′-AGTCTGGGCCCTGACCTTTTCAGACTTCTGTTTC-3′. For the *Hin*dIII-treated group, forward primer 5′-TAGCAGGAGTCTATAAAAGCGTGGAGACAG-3′ and reverse primer 5′-TGGGCAGGATTGCAGGGTTTAGAGTGG-3′ were used. For the *Pst*I-treated group, forward primer 5′-CAGCCCATTCTATAGCACTCTCCAGGAGAG-3′ and reverse primer 5′-CAGTCTCCAAACACGTAGACTGGGTATCCG-3 were used. Each 50-μL reaction mixture contained 0.4 mM of each dNTP, 25 mM $MgCl_2$, 10× LA PCR buffer II containing 20 mM Tris–HCl and 100 mM KCl, 0.5 mM primer, 2.5 U LA *Taq* polymerase and 50 ng of the processed genomic DNA. The reaction mixture of the *Eco*RI- or *Pst*I-treated group was subjected to 35 cycles of denaturation (94°C, 30 s) and annealing to extension (68°C, 8 min). For the *Hin*dIII group, the PCR conditions were denaturation (98°C, 30 s), annealing to extension (64°C, 10 min) for 5 cycles, followed by 30 cycles of denaturation (94°C, 30 s), annealing (64°C, 3 min) and extension (72°C, 15 min). Following PCR, the products were subjected to electrophoresis in 0.8% agarose gels. In the $CD3^{dim}CD7^{low}$ subpopulation from which a sufficient amount of DNA was extracted, PCR were performed in duplicate.

Cytospin and May–Giemsa staining. Cells enriched by cell sorting were washed twice with PBS. Aliquots of 100 μL of the cell suspension were mixed with 20 μL of 10% bovine serum albumin. The mixtures were centrifuged at 20*g* for 5 min onto glass slides. The fixed cells were air-dried and then subjected to May–Giemsa staining.

Statistical analyses. Data are expressed as the means ± standard deviation (SD). One-way analysis of variance (ANOVA) was used for statistical analyses, and $P < 0.05$ was taken to indicate statistical significance.

Results

Multi-color FACS, including CD3 *vs* CD7 plots, in patients with acute-type ATL. We constructed a gating procedure for flow cytometric analysis of acute-type ATL cells using a combination of CD3 and CD7. Figure 1A shows the representative flow cytometric data of an ATL sample (from patient no. 2 in Table 1). Dead cells (PI positive) were initially excluded on the forward scatter (FSC) *vs* PI plot. Next, monocytes ($CD4^{dim}$ $CD14^{+}$) were excluded on the CD4 *vs* CD14 plot. After $CD4^{+}$ T lymphocytes were gated on the CD3 *vs* CD4 plot, a CD3 *vs* CD7 plot was constructed. Based on the cell density and fluorescence intensity of CD3 and CD7, we designated three subpopulations on this plot: $CD3^{high}CD7^{high}$, $CD3^{dim}CD7^{dim}$ and $CD3^{dim}CD7^{low}$ (Fig. 1A). Using the same gating procedure, we analyzed nine patients with acute-type ATL and five normal controls (Fig. 1B). The patient characteristics analyzed in the present study are shown in Table 1. In normal controls, the expression pattern of CD3 *vs* CD7 was similar. The highest cell density was observed in the $CD3^{high}CD7^{high}$ subpopulation, and the $CD3^{dim}CD7^{dim}$ subpopulation was observed adjacent to it. The $CD3^{dim}CD7^{low}$

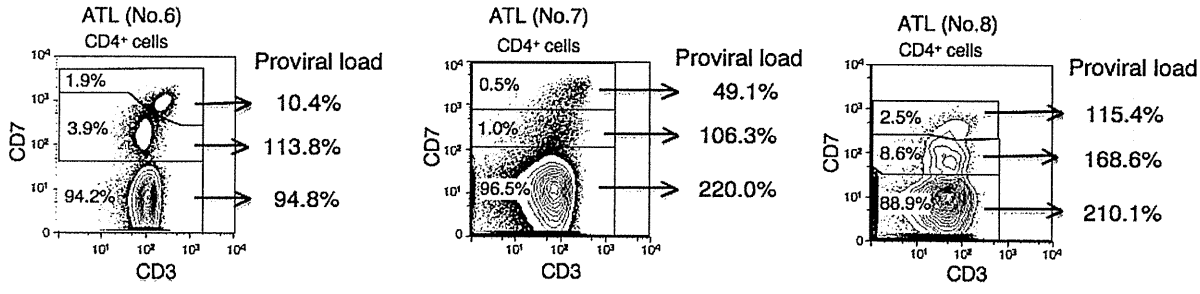

Fig. 2. Quantification of the human T-cell leukemia virus type 1 (HTLV-I) proviral load in $CD3^{high}CD7^{high}$, $CD3^{dim}CD7^{dim}$ and $CD3^{dim}CD7^{low}$ subpopulations. Genomic DNA was extracted from the FACS-sorted cells of each subpopulation and subjected to real-time quantitative PCR Representative data of three cases (patients no. 6, 7 and 8) are shown.